

LCAA, a Novel Factor Required for Magnesium Protoporphyrin Monomethylester Cyclase Accumulation and Feedback Control of Aminolevulinic Acid Biosynthesis in Tobacco^{1[W][OA]}

Christin Anne Albus², Annabel Salinas, Olaf Czarnecki, Sabine Kahlau, Maxi Rothbart, Wolfram Thiele, Wolfgang Lein³, Ralph Bock, Bernhard Grimm, and Mark Aurel Schöttler*

Max-Planck-Institut für Molekulare Pflanzenphysiologie, D-14476 Potsdam-Golm, Germany (C.A.A., S.K., W.T., W.L., R.B., M.A.S.); and Plant Physiology Group, Institute of Biology, Humboldt University Berlin, D-10115 Berlin, Germany (A.S., O.C., M.R., B.G.)

Low Chlorophyll Accumulation A (LCAA) antisense plants were obtained from a screen for genes whose partial down-regulation results in a strong chlorophyll deficiency in tobacco (*Nicotiana tabacum*). The *LCAA* mutants are affected in a plastid-localized protein of unknown function, which is conserved in cyanobacteria and all photosynthetic eukaryotes. They suffer from drastically reduced light-harvesting complex (LHC) contents, while the accumulation of all other photosynthetic complexes per leaf area is less affected. As the disturbed accumulation of LHC proteins could be either attributable to a defect in LHC biogenesis itself or to a bottleneck in chlorophyll biosynthesis, chlorophyll synthesis rates and chlorophyll synthesis intermediates were measured. *LCAA* antisense plants accumulate magnesium (Mg) protoporphyrin monomethylester and contain reduced protochlorophyllide levels and a reduced content of CHL27, a subunit of the Mg protoporphyrin monomethylester cyclase. Bimolecular fluorescence complementation assays confirm a direct interaction between *LCAA* and CHL27. 5-Aminolevulinic acid synthesis rates are increased and correlate with an increased content of glutamyl-transfer RNA reductase. We suggest that *LCAA* encodes an additional subunit of the Mg protoporphyrin monomethylester cyclase, is required for the stability of CHL27, and contributes to feedback-control of 5-aminolevulinic acid biosynthesis, the rate-limiting step of chlorophyll biosynthesis.

Photosynthetic electron transport, CO₂ fixation by the Calvin cycle, and sulfur and nitrogen assimilation all occur within the chloroplasts of photosynthetic eukaryotes, which also harbor several anabolic pathways utilizing the primary photoassimilates, such as amino acid, nucleotide, isoprenoid, and lipid synthesis. Also, the biosynthesis of several important cellular key metabolites, such as chromophores and cofactors required for photosynthesis and respiration, is localized in chloroplasts (Noctor and Foyer, 1998; DellaPenna and Pogson, 2006; Lunn, 2007; Tanaka and Tanaka, 2007; Mochizuki et al., 2010).

Chloroplasts originated from cyanobacterial ancestors but have lost most of the genes encoded by cyanobacteria during the process of endosymbiosis. In addition to tRNAs and ribosomal RNAs, only about 90 proteins are still encoded in the chloroplast genome (Kleine et al., 2009). The functions of almost all of these plastome-encoded genes have been elucidated. They are mostly involved in photosynthesis and chloroplast gene expression but also in a few other processes, such as protein turnover and fatty acid biosynthesis. The vast majority of the predicted 3,000 chloroplast proteins of higher plants are nucleus encoded. The functions of a large number of these nucleus-encoded proteins still have to be elucidated (Richly and Leister, 2004; Ferro et al., 2010; Karpowicz et al., 2011). A significant proportion of them could be involved in the biogenesis and regulation of the photosynthetic machinery. While the actual composition of the photosynthetic apparatus is well established, much less is known about factors involved in its biogenesis and regulation (Eberhard et al., 2008). As such proteins might be essential for autotrophic growth, they are difficult to identify. Usually, mutant screens of *Arabidopsis* seedlings grown on Suc-complemented medium and additional chlorophyll *a* fluorescence evaluation are employed for mutant classification (Meurer et al., 1996). These screens mainly led to the identification of mutants affected in the accumulation of the redox-active complexes of the photosynthetic electron transport chain, due

¹ This work was supported by the Max Planck Society and by the Deutsche Forschungsgemeinschaft (grant no. SFB429 A12).

² Present address: Department of Biological Chemistry, Weizmann Institute of Science, 76100 Rehovot, Israel.

³ Present address: Technische Universität Berlin, Institut für Biotechnologie, Fachgebiet Mikrobiologie, und Genetik, Gustav-Meyer-Alle 25, D-13355 Berlin, Germany.

* Corresponding author; e-mail schoettler@mpimp-golm.mpg.de.

The author responsible for distribution of materials integral to the findings presented in this article in accordance with the policy described in the Instructions for Authors (www.plantphysiol.org) is: Mark Aurel Schöttler (schoettler@mpimp-golm.mpg.de).

^[W] The online version of this article contains Web-only data.

^[OA] Open Access articles can be viewed online without a subscription.

www.plantphysiol.org/cgi/doi/10.1104/pp.112.206045

to defects in the stability and maturation of chloroplast transcripts (Felder et al., 2001; Lezhneva and Meurer, 2004), in the translation of plastid-encoded genes and the assembly of the photosynthetic complexes (Meurer et al., 1998; Stöckel and Oelmüller, 2004; Peng et al., 2006; Ma et al., 2007; Schult et al., 2007), or in cofactor insertion (Lyska et al., 2007; Schwenkert et al., 2009). However, such chlorophyll *a* fluorescence-based screens work less well to classify mutants affected in other photosynthesis-related processes, such as the accumulation of light-harvesting complex proteins (LHCs), which are the most abundant proteins in thylakoid membranes of higher plants (Kirchhoff et al., 2002). Defects in LHC accumulation do not immediately impair the function of the photosynthetic electron transport chain (Jahns and Junge, 1992) and, therefore, do not strongly alter chlorophyll *a* fluorescence properties (Hutin et al., 2002; Andersson et al., 2003).

A compromised accumulation of the nucleus-encoded LHC proteins could be attributable to multiple defects: LHC apoproteins are posttranslationally imported into the chloroplasts, and after their transport across the envelope membranes, they are bound by the chloroplast signal recognition particle (cpSRP) for transport to the thylakoid membrane. The cpSRP receptor protein cpFtsY transfers the LHC apoproteins to the membrane insertase Albino3, which catalyzes their insertion into the thylakoids (for review, see Richter et al., 2010b). While LHC accumulation is strongly impaired in single and double mutants of the two cpSRP subunits, cpSRP54 and cpSRP43, the abundance of the other photosynthetic complexes is less severely affected (Klimyuk et al., 1999; Hutin et al., 2002).

Besides defects in the cpSRP system, modest reductions of chlorophyll synthesis also specifically impair LHC protein accumulation (Falbel and Staehelin, 1994; Falbel et al., 1996; Tottey et al., 2003; Grimm, 2010). Plants ensure the assembly of sufficient amounts of core complexes of PSII and PSI by preferentially incorporating chlorophyll *a* into their reaction centers. Only when the rate of chlorophyll *a* incorporation into the reaction centers decreases do sufficient amounts of chlorophyllide *a* accumulate for efficient conversion via chlorophyllide *a* oxygenase to chlorophyll *b* (Tanaka and Tanaka, 2011). Chlorophyll *b* is not bound to the reaction centers but is essential for stable accumulation of the LHCs: in the absence of chlorophyll *b* incorporation, the LHC apoproteins are rapidly degraded (Bellemare et al., 1982; Król et al., 1995). An essential role of chlorophyll *b* for LHC stabilization was also confirmed by *in vitro* assembly studies of LHCII (Horn et al., 2007). Only a strong restriction in chlorophyll synthesis also impairs the accumulation of photosynthetic core complexes (Papenbrock et al., 2000; Hansson and Jensen, 2009; Kim et al., 2009; Dall'Osto et al., 2010). Additionally, in mutants affected in early steps of tetrapyrrole synthesis, LHC protein accumulation seems to be as strongly affected as that of the reaction centers, so that the chlorophyll *a/b* ratio remains unaltered despite the drastic reduction in total chlorophyll

content. For example, antisense repression of the glutamate-1-semialdehyde aminotransferase (GSAT) in tobacco (*Nicotiana tabacum*) resulted in strong effects on PSII and PSI, while LHC accumulation was less affected (Härtel et al., 1997). The underlying molecular basis of the differential behavior of the photosynthetic apparatus in different mutants of the tetrapyrrole biosynthesis pathway is still unknown, even though the sequence of the tetrapyrrole biosynthesis pathway has been elucidated and most enzymes involved in the pathway and their regulation have been characterized in detail (Masuda, 2008; Czarnecki and Grimm, 2012).

One notable exception is the aerobic magnesium protoporphyrin monomethylester (MgProtoMME) cyclase. It catalyzes the third specific reaction of the Mg branch of tetrapyrrole biosynthesis, leading to the formation of protochlorophyllide (Pchl_{id}), the first chlorophyll biosynthesis intermediate with the isocyclic fifth ring. In cucumber (*Cucumis sativus*), the cyclization reaction is catalyzed by a complex consisting of at least one membrane-bound and one soluble protein located in the chloroplast stroma (Wong and Castelfranco, 1984). Based on its partial biochemical purification, the soluble component was suggested to have a molecular mass of over 30 kD (Walker et al., 1991). *AcsF* (for aerobic cyclization system iron-containing protein) from *Rubrivivax gelatinosus* was the first identified gene encoding an oxidative cyclase component (Pinta et al., 2002). Subsequently, homologous genes were found in all investigated aerobic photoautotrophic organisms, such as *Crd1* and *Cth1* in *Chlamydomonas reinhardtii* (Moseley et al., 2002) and *cyclII* and *chlA1/2* in *Synechocystis* sp. PCC 6803 (Minamizaki et al., 2008; Peter et al., 2009). In *Arabidopsis* (*Arabidopsis thaliana*), the homologous diiron protein CHL27 was identified as the membrane-associated catalytic subunit of the cyclase. It is equally associated with the inner envelope and the thylakoid membrane (Tottey et al., 2003). This distribution was also confirmed for the barley (*Hordeum vulgare*) homolog of CHL27, Xantha-I (Rzeznicka et al., 2005). Additionally, in barley, genetic evidence for a second membrane-bound cyclase component, whose molecular identity is still unknown, was obtained in the *viridis-k* mutant (Gough, 1972; Rzeznicka et al., 2005). CHL27 resembles a subunit of monooxygenase-related proteins (Berthold and Stenmark, 2003), which usually consist of a catalytic subunit, a reducing subunit, and a scaffold subunit. Because CHL27 is likely the substrate-binding catalytic subunit, the reducing and scaffold subunits still need to be identified. The NADPH-dependent thioredoxin reductase (NTRC) was shown to protect the activity of the cyclase (Stenbaek et al., 2008); however, whether NTRC indeed is one of the missing subunits of the aerobic cyclase is still a matter of debate.

Because tetrapyrrole biosynthesis is not only required for the supply of chlorophyll but also of heme, siroheme, and phytylchromobilin (Tanaka and Tanaka, 2007; Czarnecki and Grimm, 2012), it is essential both under autotrophic and mixotrophic growth conditions,

so that mutations resulting in the complete abolishment or massive deregulation of tetrapyrrole biosynthesis are lethal to plants (Mochizuki et al., 2010; Czarnecki and Grimm, 2012). To identify genes involved in such essential cellular functions, transgenic approaches enabling a gradual repression of gene expression can be employed. Lein and coworkers (2008) used a normalized complementary DNA (cDNA) library from tobacco leaves to generate a large collection of tobacco antisense transformants. These transformants were then screened for strong defects in leaf pigmentation and autotrophic growth. This screen led to the identification of several well-known proteins involved in photosynthesis and primary metabolism, but it also identified nine proteins of unknown function, for which an important role in plant growth and cell viability was established. In a previous publication, we showed that one of these unknown proteins, Ycf3-interacting protein1, is a novel assembly factor required for PSI biogenesis (Albus et al., 2010). Here, we have analyzed another protein of unknown function identified in this screen, whose antisense repression results in a strong reduction in leaf pigmentation. While pigmentation mutants predominantly affected in the biogenesis of photosynthetic reaction centers are characterized by a stronger repression of chlorophyll *a* than of chlorophyll *b* accumulation, the *Low Chlorophyll Accumulation A* (*LCAA*) antisense plants show a stronger reduction in chlorophyll *b* content relative to chlorophyll *a* and an impaired accumulation of LHC proteins. We show that this is attributable to a general repression of chlorophyll biosynthesis, due to a defect in the oxidative cyclase reaction. A role of *LCAA* as a novel protein factor involved in the catalytic reaction of the cyclase is discussed.

RESULTS

To identify genes for critical and potentially essential functions, whose partial repression results in a strong chlorophyll deficiency and retardation of photoautotrophic

growth, Lein et al. (2008) used a normalized cDNA library from tobacco leaves to generate a large collection of tobacco antisense transformants. Here, we have analyzed the function of an unknown protein identified in this screen in detail. We characterized four independent antisense lines against the *LCAA* gene. The four lines, *LCAA1* to *LCAA4*, were numbered in the order of increasing severity of their phenotypes (Fig. 1A). The photograph was taken when the wild type started to form flower buds. All antisense lines were retarded in growth relative to the wild type, and pigment deficiency was increasingly pronounced. Accumulation of the *LCAA* mRNA was reduced in all antisense lines relative to the wild type (Fig. 1B).

LCAA Is a Highly Conserved Plastid-Localized Protein

We checked for homologs of the silenced tobacco gene, which encodes a protein of 222 amino acids in length. The orthologous gene in *Arabidopsis* is At5g58250, which encodes a protein of 211 amino acids. Homologs are found in all photosynthetic eukaryotes and in cyanobacteria. All homologous protein sequences share the Ycf54 domain, a domain of unknown function (also called DUF2488 in the Pfam database; <http://pfam.sanger.ac.uk/>). In Figure 2, a sequence alignment of the tobacco and *Arabidopsis LCAA* genes with their homolog from the green alga *C. reinhardtii* is shown. Additionally, plastome-encoded homologs from the moss *Physcomitrella patens*, the red alga *Porphyra purpurea*, the brown alga *Fucus vesiculosus*, and *Paulinella chromatophora* (a freshwater amoeboid that established its endosymbiosis with a cyanobacterium in a phylogenetically independent event from all other photosynthetic eukaryotes) were included. Finally, sequences from two cyanobacteria (*Synechococcus* sp. WH8102 and *Nostoc punctiforme* PCC 73102) were aligned. The partial evolutionary retention of the *LCAA* gene in the plastome already suggests a function of *LCAA* in the chloroplast. Additionally, both IPSORT (Bannai et al., 2002; <http://ipsort.hgc.jp/>) and TargetP V1.1 (Emanuelsson et al., 2007; <http://www.cbs.dtu.dk/services/TargetP/>) support this localization for the higher



Figure 1. A, Growth phenotypes of tobacco wild type (WT) and the four *LCAA* antisense lines in the order of increasing strength of the phenotype. Plants were grown in the greenhouse at $250 \mu\text{E m}^{-2} \text{s}^{-1}$ actinic light intensity. B, Northern blot showing the correlation between the visible phenotype and *LCAA* mRNA accumulation.

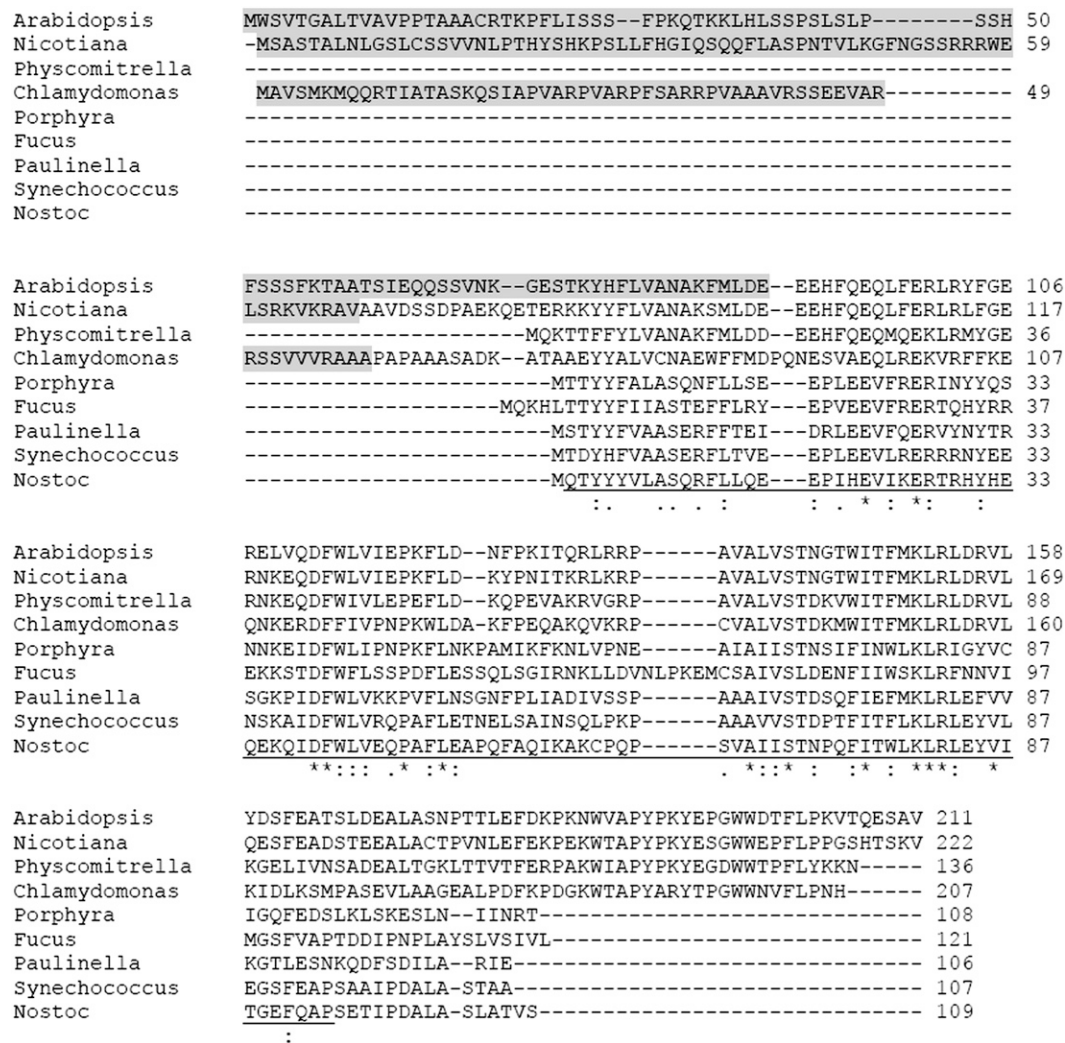


Figure 2. Sequence alignment showing the evolutionary conservation of LCAA in higher plants, mosses, eukaryotic algae, and cyanobacteria. The homologs from tobacco, Arabidopsis, and *C. reinhardtii* are nucleus encoded and therefore possess a putative chloroplast transit peptide at their N terminus. The LCAA homologs of the moss *P. patens*, the red alga *P. purpurea*, the brown alga *F. vesiculosus*, and *P. chromatophora* are all plastid encoded and therefore lack an N-terminal transit peptide. Additionally, sequences from two cyanobacteria (*Synechococcus* sp. WH8102 and *N. punctiforme* PCC 73102) were included. Identical amino acids are marked by stars, conserved substitutions by colons, and semiconserved substitutions by dots. The seed sequence of the Ycf54 domain (DUF2488) is underlined.

plant proteins. LCAA has been identified as a chloroplast-localized protein in the Plant Proteomics Database at Cornell (Sun et al., 2009; <http://ppdb.tc.cornell.edu/>) and is suggested to be associated with the thylakoid membrane. To experimentally confirm the chloroplast localization of LCAA, we constructed fusions of GFP with the Arabidopsis and the tobacco *LCAA* genes. The fusion constructs were transiently transformed into tobacco protoplasts and expressed under the control of the strong constitutive cauliflower mosaic virus 35S promoter. Confocal laser scanning microscopy and overlays of GFP and chlorophyll *a* fluorescence revealed that both the tobacco and Arabidopsis proteins are targeted to the chloroplast, while the GFP control is clearly retained in the cytosol (Fig. 3).

LHC Accumulation Is Strongly Reduced in the *LCAA* Antisense Plants

As the localization in the chloroplast and the pigment-deficient phenotype of the *LCAA* antisense plants indicated a direct or indirect role of LCAA in photosynthesis, we performed a detailed analysis of the photosynthetic apparatus of the tobacco transformants. As shown in Table I, the chlorophyll content was strongly reduced in the antisense plants. Antisense line *LCAA4*, with the strongest pale-green phenotype, contained less than 15% of wild-type chlorophyll levels. Accumulation of chlorophyll *b* was much more affected than chlorophyll *a* accumulation, as shown by the drastic increase of the chlorophyll *a/b* ratio from 3.92 in the wild type to 15.38

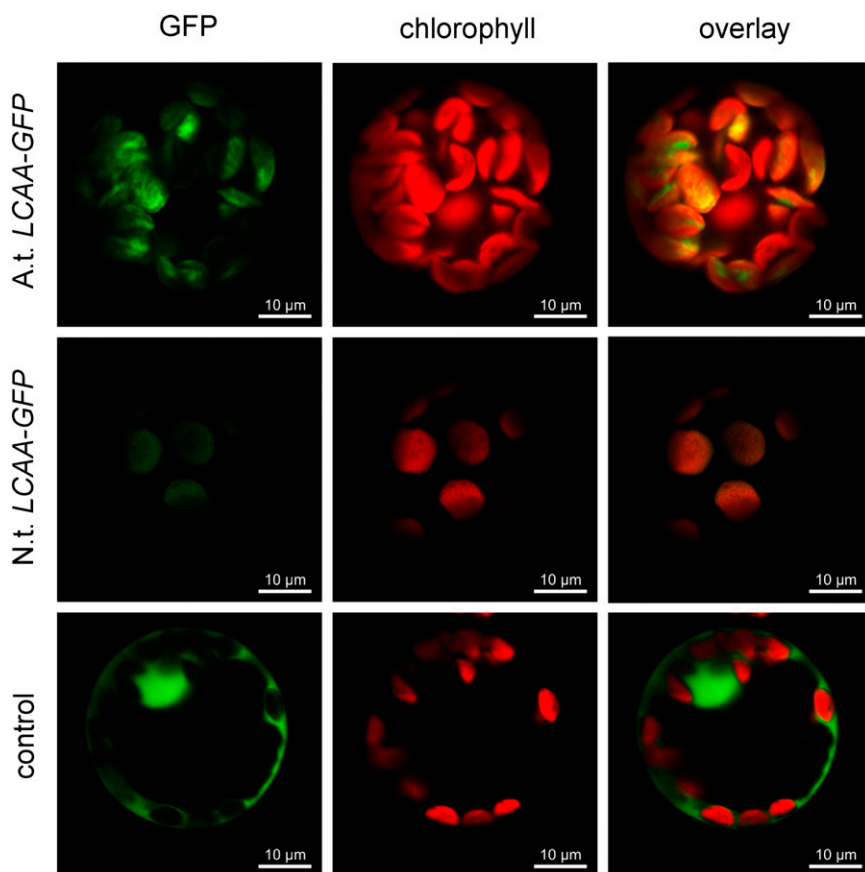


Figure 3. Targeting of LCAA to chloroplasts. Fusions of GFP with the Arabidopsis and the tobacco *LCAA* genes were transiently transformed into tobacco protoplasts and expressed under the control of the strong constitutive cauliflower mosaic virus 35S promoter. Confocal laser scanning microscopy and overlays of GFP and chlorophyll *a* fluorescence revealed that both the tobacco and Arabidopsis proteins are targeted to the chloroplast, while the unfused GFP control is clearly retained in the cytosol.

in *LCAA4*. As chlorophyll *b* is exclusively bound to the LHC proteins, while the reaction centers only bind chlorophyll *a*, these data point to a reduced LHC accumulation. Despite the drastically reduced chlorophyll content, the effect on leaf absorptance was relatively small (Table I). Other parameters, such as the maximum quantum efficiency of PSII, light- and CO_2 -saturated assimilation capacity, and respiration, were unaffected in spite of the drastic reduction in chlorophyll *b* accumulation (Table I). These observations are well consistent with a defect in LHC accumulation, as a reduced antenna cross-section of the photosystems should not alter the leaf assimilation capacity under light-saturated conditions. Also, as long as the function of the reaction center of PSII is not directly impaired, changes in antenna cross sections do not alter its maximum quantum efficiency, as shown previously for several LHCII-deficient mutants (Hutin et al., 2002; Andersson et al., 2003). However, the maximum quantum efficiency of CO_2 -saturated assimilation, as determined in the linear range of the light response curve between 0 and $80 \mu\text{E m}^{-2} \text{s}^{-1}$ light intensity, was strongly reduced in the antisense lines. While in the wild type, on average 12.4 quanta were needed for the assimilation of one molecule of CO_2 , the quantum demand increased more than 2-fold in the palest antisense line. As a consequence, at the growth light intensity ($250 \mu\text{E m}^{-2} \text{s}^{-1}$), leaf assimilation was severely reduced in all antisense lines, from $15.8 \mu\text{mol CO}_2 \text{ m}^{-2} \text{s}^{-1}$ in the wild

type to only $6.3 \mu\text{mol CO}_2 \text{ m}^{-2} \text{s}^{-1}$ in the most severely affected line, *LCAA4*. This cannot be explained by the reduced leaf absorptance alone and points to additional problems in electron transport under light-limited conditions (see below).

We quantified the components of the photosynthetic electron transport chain in isolated thylakoids using spectroscopic approaches. The contents were then normalized both to a chlorophyll and a leaf area basis (Table II). In line with a predominant defect in LHC accumulation, on a chlorophyll basis contents of PSII were almost 3-fold increased, while cytochrome *b₆f* complex contents were 4-fold higher in the strongest antisense line in comparison with the wild type. In the case of plastocyanin, the increase was even more pronounced. PSI accumulation was only moderately increased. As a consequence, on a leaf area basis, moderate reductions in cytochrome *b₆f* complex and plastocyanin contents were observed, while PSII and especially PSI contents were more strongly diminished.

These spectroscopic data were confirmed by immunoblots against representative subunits of the different photosynthetic complexes (Fig. 4A). Samples were loaded on an equal chlorophyll basis, and for semiquantitative analysis, 200%, 150%, and 100% of the wild-type sample were loaded in lanes 1 to 3 for comparison. Immunodetection of the essential PSII reaction center subunits PsbD (D2 protein) and PsbE

Table I. Various parameters in the wild type and in the different LCAA antisense lines

Plants were grown in the greenhouse at approximately 250 $\mu\text{E m}^{-2} \text{s}^{-1}$ actinic light intensity. All measurements were performed on the youngest fully expanded leaves of plants at the onset of flowering. For each antisense line, a minimum of four plants were measured, and data were subjected to one-way ANOVA using a pairwise multiple comparison procedure (Holm-Sidak method) in SigmaPlot. Boldface values are significantly different from the wild type.

Parameter	Wild Type	LCAA1	LCAA2	LCAA3	LCAA4
Chlorophyll <i>a/b</i> ratio	3.92 \pm 0.07	6.26 \pm 0.41	7.47 \pm 1.12	8.95 \pm 1.36	15.38 \pm 5.27
Chlorophyll content (mg m^{-2})	469.3 \pm 14.8	255.5 \pm 16.1	130.9 \pm 33.3	87.2 \pm 19.7	58.5 \pm 8.5
Leaf absorptance (%)	90.9 \pm 0.9	90.9 \pm 1.2	82.9 \pm 2.9	71.1 \pm 0.4	65.1 \pm 9.8
Maximum quantum efficiency of PSII in the dark-adapted state	0.80 \pm 0.01	0.81 \pm 0.01	0.80 \pm 0.01	0.79 \pm 0.01	0.78 \pm 0.01
Assimilation capacity ($\mu\text{mol CO}_2 \text{ m}^{-2} \text{ s}^{-1}$)	25.5 \pm 3.8	26.8 \pm 2.0	26.2 \pm 1.9	24.7 \pm 2.1	25.4 \pm 3.7
Assimilation at 250 $\mu\text{E m}^{-2} \text{ s}^{-1}$ ($\mu\text{mol CO}_2 \text{ m}^{-2} \text{ s}^{-1}$)	15.8 \pm 2.1	10.4 \pm 0.6	9.6 \pm 0.5	7.7 \pm 1.3	6.3 \pm 0.5
Respiration ($\mu\text{mol CO}_2 \text{ m}^{-2} \text{ s}^{-1}$)	-1.2 \pm 0.5	-1.2 \pm 0.2	-1.0 \pm 0.1	-1.0 \pm 0.1	-0.9 \pm 0.1
Quanta per CO_2	12.4 \pm 1.9	16.7 \pm 1.0	18.6 \pm 1.4	23.6 \pm 6.6	28.2 \pm 5.5

(α -subunit of cytochrome b_{559}) confirmed the strong increase in PSII accumulation per chlorophyll, which was most pronounced in the palest antisense line, LCAA4. Also, the contents of the extrinsic PsbO subunit of the oxygen-evolving complex and of the nonessential PsbS protein, which belongs to the LHC protein superfamily and is required for photoprotective nonphotochemical quenching of excess excitation energy (Jansson, 1999; Engelken et al., 2010), showed a comparable increase. Cytochrome b_6f complex accumulation was probed with antibodies against cytochrome *f* (PetA) and the Rieske iron-sulfur protein (PetC). Its strong increase especially in lines LCAA3 and LCAA4 was confirmed. PSI accumulation was probed with antibodies against the essential PsA and PsB reaction center subunits. In line with the spectroscopic data, the PSI reaction center was less than 2-fold increased in all antisense lines. Finally, ATP synthase abundance was probed with an antibody against the essential AtpB subunit. Similar to PSII and the cytochrome b_6f complex, also ATP synthase accumulation per chlorophyll was strongly increased in the LCAA antisense plants.

Next, we determined the accumulation of several LHCI and LHCII proteins by immunoblotting. Again, equal amounts of chlorophyll were loaded (Fig. 4B). A

dilution series of 25%, 50%, and 100% of the wild-type sample was loaded in lanes 1 to 3 for semiquantitative analysis. For the PSII antenna, accumulation of the Lhcb1 and Lhcb2 subunits, which are both part of the trimeric LHCI complexes, was tested. For the PSI antenna, accumulation of Lhca1, Lhca2, and Lhca4 was determined. The accumulation of all LHC proteins was somewhat diminished in the antisense lines, with the effects being most pronounced in antisense line 4, in agreement with its strongest increase in the chlorophyll *a/b* ratio. Among the LHCI proteins, Lhca1 and Lhca4 were more strongly affected than Lhca2. This is in line with previous reports on reduced LHC contents in mutants with diminished synthesis of chlorophyll *b* (Król et al., 1995; Bossmann et al., 1997).

Finally, to directly assess effects of the decreased LHC accumulation on the antenna cross sections of the photosystems, 77K chlorophyll *a* fluorescence emission spectra were recorded (Fig 5A). The signals were normalized to the emission peak of PSII-LHCI at 686 nm wavelength. In the antisense plants, the emission peak of PSI-LHCI was slightly blue shifted from 733 nm in the wild type to 730 nm in the strongly affected mutant lines, which is similar to spectral changes in *Lhca* antisense plants with reduced accumulation of

Table II. Photosynthetic complex accumulation on a chlorophyll and leaf area basis

Averages and SD values of photosynthetic complex accumulation per mol chlorophyll (top part of the table) and per m^{-2} leaf area (bottom part of the table) are shown for the wild type and the four different LCAA antisense lines. PSII contents were calculated from difference absorbance signals of cytochrome b_{559} , cytochrome b_6f complex contents from difference absorbance signals of cytochrome *f* and cytochromes b_6 , and PSI contents from P_{700} difference absorbance signals. Data were subjected to one-way ANOVA using a pairwise multiple comparison procedure (Holm-Sidak method) in SigmaPlot. Boldface values are significantly different from the wild type.

Parameter	Wild Type	LCAA1	LCAA2	LCAA3	LCAA4
PSII (mmol mol^{-1} chlorophyll)	2.65 \pm 0.17	3.95 \pm 0.47	5.16 \pm 0.70	6.11 \pm 0.55	7.42 \pm 0.43
Cytochrome b_6f complex (mmol mol^{-1} chlorophyll)	1.23 \pm 0.05	2.21 \pm 0.23	3.06 \pm 0.53	3.94 \pm 0.42	4.78 \pm 0.60
Plastocyanin (mmol mol^{-1} chlorophyll)	5.35 \pm 0.84	9.34 \pm 0.81	17.39 \pm 3.63	26.88 \pm 5.26	28.47 \pm 1.68
PSI (mmol mol^{-1} chlorophyll)	2.36 \pm 0.05	2.82 \pm 0.12	2.99 \pm 0.08	3.05 \pm 0.09	2.81 \pm 0.10
PSII ($\mu\text{mol m}^{-2}$)	1.24 \pm 0.09	1.01 \pm 0.17	0.66 \pm 0.11	0.52 \pm 0.09	0.43 \pm 0.05
Cytochrome b_6f complex ($\mu\text{mol m}^{-2}$)	0.58 \pm 0.04	0.57 \pm 0.09	0.38 \pm 0.05	0.34 \pm 0.07	0.28 \pm 0.03
Plastocyanin ($\mu\text{mol m}^{-2}$)	2.50 \pm 0.35	2.39 \pm 0.30	2.17 \pm 0.31	2.29 \pm 0.51	1.65 \pm 0.16
PSI ($\mu\text{mol m}^{-2}$)	1.11 \pm 0.04	0.72 \pm 0.05	0.39 \pm 0.09	0.27 \pm 0.06	0.16 \pm 0.03

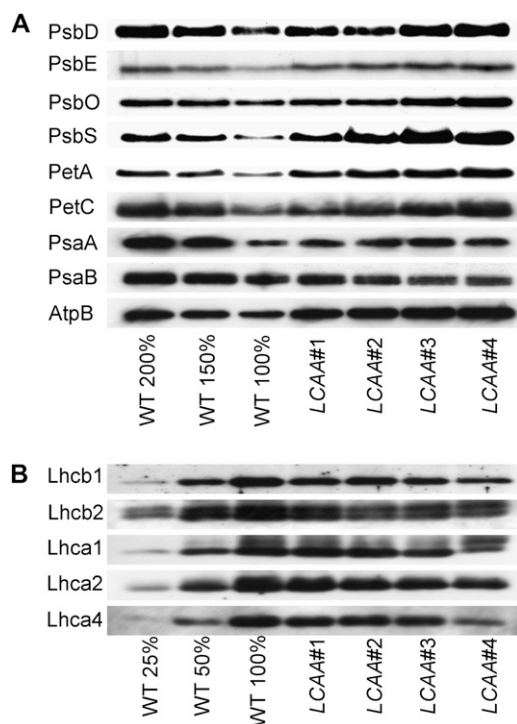


Figure 4. Accumulation of photosynthetic complexes and antenna proteins, as quantified by immunoblot analyses using antibodies against essential subunits of the different photosynthetic complexes (A) and representative antenna proteins of PSII and PSI (B). A, Samples were loaded on an equal chlorophyll basis, and for semiquantitative analysis, 200%, 150%, and 100% of the wild-type sample (WT) were loaded in lanes 1 to 3 for comparison. For PSII, the essential PSII reaction center subunits PsbD (D2 protein) and PsbE, the extrinsic PsbO subunit of the oxygen-evolving complex, and the nonessential PsbS protein, which is required for photoprotective nonphotochemical quenching of excess excitation energy, were analyzed. Cytochrome b_6/f complex accumulation was probed with antibodies against cytochrome f (PetA) and the Rieske iron-sulfur protein (PetC). PSI accumulation was probed with antibodies against the essential PsaA and PsaB reaction center subunits. ATP synthase abundance was probed with an antibody against the essential AtpB subunit. B, To determine LHC protein accumulation, a dilution series of 25%, 50%, and 100% of the wild-type sample was loaded in lanes 1 to 3 for semiquantitative analysis. For the PSII antenna, accumulation of the Lhcb1 and Lhcb2 subunits was tested. For the PSI antenna, accumulation of Lhca1, Lhca2, and Lhca4 was determined.

different Lhca proteins (Zhang et al., 1997; Ganeteg et al., 2001). Additionally, the chlorophyll a fluorescence emission peak from the PSI-LHCI supercomplex was diminished relative to the emission peak from PSII-LHCII. This is in line with a reduced accumulation of the antenna proteins and with the increased ratio of PSII to PSI shown in Figure 4A and Table II. Light-response curves of the chlorophyll a fluorescence parameter q_L , a measure of the redox state of the PSII acceptor side, reveal a faster reduction of the PSII acceptor side at low actinic light intensities in the strong antisense lines than in the wild type (Fig. 5B). This observation is consistent with the changes in

photosystem stoichiometry and total antenna cross-sections, as it can be most easily explained by an overexcitation of PSII relative to PSI. This imbalanced excitation could also contribute to the decreased quantum efficiency of CO_2 assimilation (Table I). Light response curves of q_N , a measure for nonphotochemical quenching of excess excitation energy, revealed a reduced maximum q_N under light-saturated conditions in the most strongly affected antisense lines (Fig. 5C). Consistent with nonphotochemical quenching occurring within the PSII antenna system, a reduced maximum q_N capacity has been reported previously for several LHC-deficient mutants (Havaux et al., 2007; Hansson and Jensen, 2009).

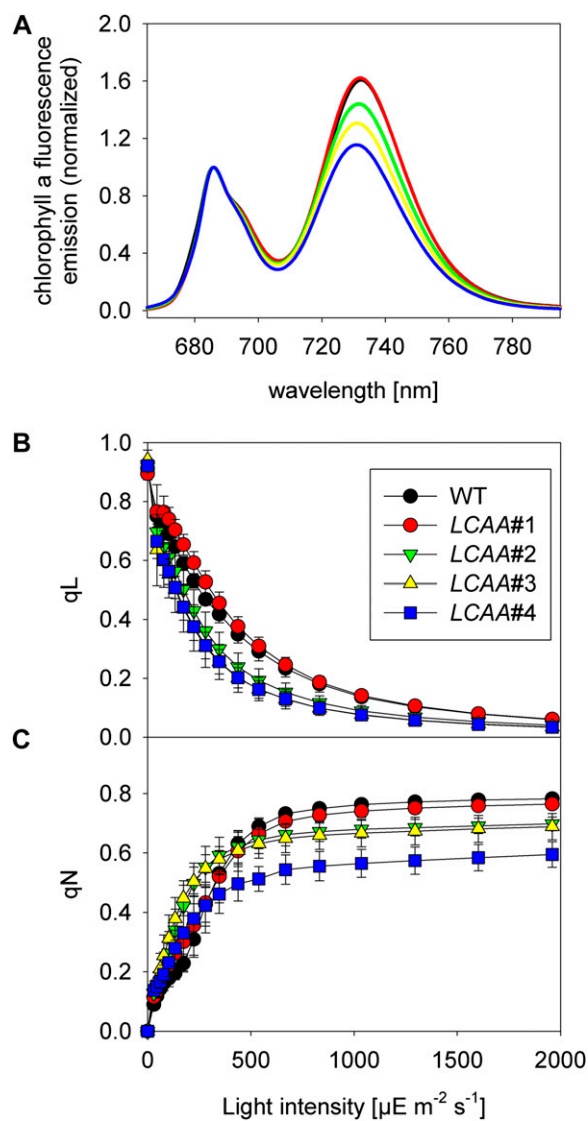


Figure 5. Chlorophyll a fluorescence data to analyze antenna function. A, 77K chlorophyll a fluorescence emission spectra. The emission maximum of PSII-LHCII at 686 nm was normalized to 1. B, Light-response curve of q_L . The fully oxidized state of the PSII acceptor side was normalized to 1, and the fully reduced state was normalized to 0. C, Light-response curve of q_N . WT, Wild type.

LCAA Is Required for the Mg Protoporphyrin IX Monomethylester Oxidative Cyclase

The reduced content of LHC proteins could be explained by a defect in the biogenesis or membrane insertion of LHC apoproteins or by a defect in chlorophyll biosynthesis. Perturbations in the metabolic pathway of tetrapyrrole biosynthesis can be determined by quantifications of pathway intermediates. To identify the rate-limiting step in the chlorophyll-synthesizing branch of the pathway in the *LCAA* antisense plants, leaf discs of *LCAA* antisense and wild-type seedlings were incubated with 1 mM 5-aminolevulinic acid (ALA) for 24 h in low light. ALA feeding helps to circumvent the general control of tetrapyrrole synthesis rates by glutamyl-transfer RNA reductase (GluTR), which catalyzes the first committed step of the tetrapyrrole biosynthetic pathway and is usually repressed in response to a limitation further downstream in the pathway (Papenbrock et al., 2000; Meskauskiene et al., 2001; Moulin and Smith, 2005; Shalygo et al., 2009; Czarnecki and Grimm, 2012).

After ALA feeding, the chlorophyll precursors magnesium protoporphyrin IX (MgProtoIX), MgProtoMME, and Pchlide were analyzed by HPLC. MgProtoIX, MgProtoMME, and Pchlide are the substrates of Mg protoporphyrin methyltransferase, of the cyclase, and of NADPH-Pchlide oxidoreductase (POR), respectively. The ALA supply was low enough to exclude additional negative photooxidative effects during the incubation time. The *LCAA* antisense lines accumulated excessive amounts of MgProtoMME and MgProtoIX in comparison with wild-type plants (Table III). Despite its more severe phenotype, line *LCAA4* accumulated somewhat lower amounts of MgProtoIX and MgProtoMME than line *LCAA3*. The antisense lines also showed reduced levels of Pchlide, whose decrease paralleled the pigment-deficient phenotype.

Having confirmed that excessive amounts of Mg porphyrins can easily be quantified upon ALA feeding, also steady-state levels of Mg porphyrins were analyzed in the *LCAA* antisense lines (Table IV). HPLC analyses revealed a similar difference in the Mg porphyrin contents between wild-type and transgenic seedlings to those observed after ALA feeding. The MgProtoMME steady-state levels increased in the *LCAA* antisense lines relative to wild-type plants, and line 3 accumulated the highest amount of MgProtoMME. The reduction in chlorophyll contents correlated inversely with the accumulation of MgProtoMME in the *LCAA* antisense plants, except for the most severely affected line, *LCAA4*. The steady-state levels of Pchlide in light-grown transgenic *LCAA* lines were diminished in comparison with control plants (Table IV). The Pchlide levels were also determined in *LCAA* lines and control plants after 15 h of incubation in darkness. The dark-grown plants accumulated approximately 10 times more Pchlide relative to the steady-state content in light. The *LCAA*

Table III. Average concentrations and SD values of chlorophyll precursors (Mg porphyrins and Pchlide) of tobacco wild type and the four *LCAA* antisense lines after ALA (1 mM) feeding for 24 h

Plant	MgProtoIX	MgProtoMME	Pchlide
	<i>pmol g⁻¹ fresh wt</i>		
Wild type	29 ± 5	120 ± 50	440 ± 325
<i>LCAA1</i>	57 ± 12	531 ± 376	363 ± 305
<i>LCAA2</i>	109 ± 128	1,031 ± 1,287	331 ± 16
<i>LCAA3</i>	1,417 ± 902	5,658 ± 241	300 ± 91
<i>LCAA4</i>	301 ± 77	3,571 ± 806	182 ± 21

lines again showed the gradually reduced Pchlide accumulation in darkness, down to less than 20% of wild-type content in line *LCAA4* (Table IV).

Measuring the ALA synthesis rate of tobacco leaves indicated that *LCAA* antisense plants possess a higher synthesis rate than wild-type plants (Fig. 6A). To elucidate the molecular basis of this increased capacity, the accumulation of key enzymes of tetrapyrrole biosynthesis was determined by immunoblotting. Total protein was extracted from leaves, and equal protein amounts were loaded. The increased ALA-synthesizing capacity corresponds with elevated GluTR levels (Fig. 6B). Additionally, a gradually increased content of the Mg chelatase subunit CHLH, the Mg protoporphyrin methyltransferase (CHLM), and POR could be determined compared with the wild type and reversely corresponds to reduced chlorophyll contents of the transgenic *LCAA* lines. In contrast, the content of CHL27, which is required for the cyclase reaction, decreases in the *LCAA* lines in comparison with the control. Lower CHL27 contents are indicative of a reduced cyclase reaction (Totter et al., 2003; Peter et al., 2010). The contents of GSAT and the Mg chelatase subunit CHLD were not altered in the *LCAA* lines in comparison with control plants, indicating altered enzyme contents only in specific steps of tetrapyrrole biosynthesis, while other enzymatic steps were not affected in response to reduced *LCAA* expression. We also included LIL3 and NTRC to the protein analysis. LIL3 is a member of the LHC-like protein family, which interacts with and stabilizes the geranylgeranyl reductase involved in the late steps of chlorophyll biosynthesis (Tanaka et al., 2010). NTRC was suggested to protect the aerobic cyclase against oxidative stress (Stenbaek et al., 2008). Except for the most strongly affected antisense line 4, *LCAA* lines contain elevated LIL3 and NTRC contents, which parallel the contents of GluTR, CHLM, CHLH, and POR.

Expression of Genes for Tetrapyrrole Biosynthesis Enzymes Is Up-Regulated in *LCAA* Antisense Plants

To understand the molecular basis of the increased accumulation of most of the proteins involved in tetrapyrrole biosynthesis in the *LCAA* antisense lines (Fig. 6B), we determined transcript abundances for 23 genes encoding components of the tetrapyrrole

Table IV. Average concentrations and *sd* values of steady-state levels of chlorophyll precursors (Mg porphyrins and Pchlide) of tobacco wild type and the four LCAA antisense lines

The samples for Pchlide analysis in darkness were harvested after a 15-h dark period.

Plant	MgProtoIX	MgProtoMME	Pchlide	Pchlide (Dark)
	<i>pmol g⁻¹ fresh wt</i>			
Wild type	24 ± 11	11 ± 3	678 ± 149	6,156 ± 674
<i>LCAA1</i>	55 ± 19	252 ± 187	309 ± 34	4,499 ± 610
<i>LCAA2</i>	163 ± 97	2,110 ± 1,883	400 ± 88	4,213 ± 646
<i>LCAA3</i>	451 ± 72	3,994 ± 904	127 ± 11	1,878 ± 645
<i>LCAA4</i>	125 ± 26	1,261 ± 305	133 ± 16	1,163 ± 200

biosynthetic pathway via quantitative PCR (qPCR) analysis. While in most cases, transcript levels in the weak antisense lines *LCAA1* and *LCAA2* were not significantly different from the wild type, the stronger antisense lines *LCAA3* and especially *LCAA4* displayed a significant up-regulation of all tested genes encoding tetrapyrrole biosynthesis enzymes (Fig. 7A). Transcript accumulation was most strongly increased in antisense line *LCAA4*, which suffers from the most severe growth retardation. The most pronounced, approximately 8-fold increase in transcript accumulation in line *LCAA4* was observed for *PorA* and *PorB*, encoding two isoforms of the NADPH-dependent protochlorophyllide oxidoreductase, while expression of the third POR encoded by *PorC* was only 3-fold increased. Expression of *Chl27*, whose protein content was strongly diminished in the antisense lines (Fig. 6B), was weakly but significantly up-regulated in the antisense lines, suggesting that the specific loss of CHL27 is not attributable to a specific repression of its gene expression.

Additionally, also the expression of several LHC isoforms, of nucleus-encoded subunits of the different photosynthetic complexes, and of proteins of the antioxidative system of the chloroplast was determined (Fig. 7B). Despite the decreased accumulation of the LHC proteins, expression of *Lhca1*, *Lhca6*, *Lhcb2*, *Lhcb3*, and *Lhcb6* was increased 2- to 3-fold in the strong antisense line *LCAA4*, and for antisense line *LCAA3*, a similar (although somewhat weaker) tendency toward increased transcript abundances was found, clearly showing that decreased LHC protein accumulation cannot be attributed to decreased gene expression. Also for *AtpD* (encoding the δ -subunit of chloroplast ATP synthase), *PetC* (encoding the essential Rieske iron-sulfur protein of the cytochrome *b₆f* complex), and the two isoforms of *PsbO* and *PsaD*, an approximately 2-fold increase in transcript accumulation was found in the strongest antisense line. Two genes encoding enzymes of the antioxidative system in the chloroplast, *Apx* (for ascorbate peroxidase) and *Fsd1* (the major chloroplast isoform of the superoxide dismutase), were also significantly up-regulated in the antisense lines *LCAA3* and *LCAA4*.

Bimolecular Fluorescence Complementation Assays Suggest a Direct Interaction between LCAA and CHL27

As the specific loss of CHL27 protein accumulation in the stronger antisense lines cannot be attributed to

repressed *Chl27* gene expression, we next considered the possibility that a direct protein-protein interaction between LCAA and CHL27 is necessary for the stable accumulation of the CHL27 subunit of the cyclase. Therefore, we used bimolecular fluorescence complementation to test for a physical interaction of both proteins (Fig. 8). To this end, the coding regions of *LcaA* and *Chl27* were fused to the N- and C-terminal halves of the enhanced VENUS variant of the yellow fluorescent protein (Waadt et al., 2008). After transient cotransformation of the constructs into *Nicotiana benthamiana* leaves (Gehl et al., 2009), restored yellow fluorescent protein fluorescence was observed in chloroplasts of transformants expressing both LCAA and CHL27, while no fluorescence was restored when the two halves of VENUS were fused to CHL27 alone, indicating that CHL27 does not form homodimers. Interestingly, when both halves of VENUS were fused to LCAA, again, a fluorescence signal was restored, suggesting that in addition to interaction with CHL27, LCAA also forms homodimers.

DISCUSSION

The genomes of higher plants encode 25,000 to 35,000 different proteins, and the functions of the vast majority of these proteins have not been assigned to date. Even the functions of more than one-half of the approximately 3,000 proteins located within the chloroplast, which arguably is the most in-depth characterized plant organelle, are still unknown. The identification and characterization of essential proteins of unknown function in higher plants is especially difficult, as knockout mutations will be lethal and cannot be rescued by growth under mixotrophic conditions. Therefore, Lein and coworkers (2008) generated a large collection of tobacco antisense plants, which they screened for transformants displaying a strong chlorotic phenotype and retarded growth. In tobacco, the antisense repression of target genes is typically much less severe than gene silencing achieved by RNA interference approaches. Thus, this screen was expected to allow the identification of proteins whose partial repression already results in strong physiological defects. The identified candidates should exert strong control of essential metabolic and cellular processes. Besides many known gene products, also several unknown proteins were identified in that screen

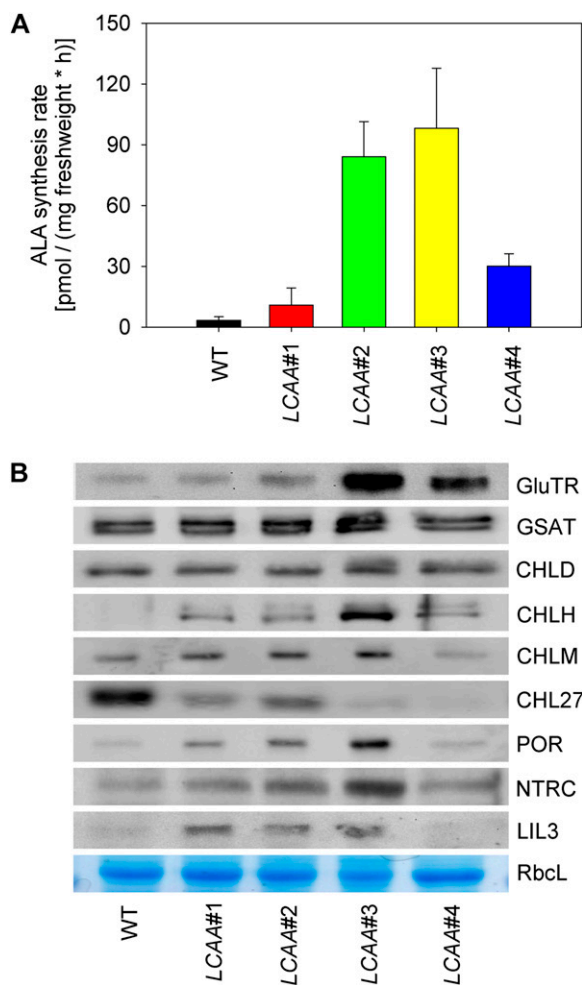


Figure 6. ALA synthesis rate and accumulation of key enzymes of tetrapyrrole biosynthesis. **A**, ALA synthesis rates as determined in tobacco leaf discs after incubation in 40 mM levulinic acid under continuous white light ($120 \mu\text{E m}^{-2} \text{s}^{-1}$) at 22°C for 4 h. *LCAA* mutants possess a higher ALA synthesis rate than control tobacco plants. **B**, Immunoblots against representative enzymes of the tetrapyrrole biosynthesis pathway. Total protein was extracted from leaves, and equal protein amounts were loaded. The measured enzymes are GluTR, GSAT, the Mg chelatase subunit CHLD, the CHLH subunit of the Mg chelatase, the CHLM subunit of the Mg protoporphyrin methyltransferase, the CHL27 subunit of the MgProtoMME cyclase, and POR. Additionally, LIL3 and NTRC were included. LIL3 stabilizes the geranylgeranyl reductase involved in the late steps of chlorophyll biosynthesis, and NTRC protects the MgProtoMME cyclase against oxidative stress. *LCAA* antisense lines contain elevated LIL3 and NTRC contents, which parallel the increased contents of GluTR, CHLH, CHLM, and POR. WT, Wild type.

and later functionally characterized (Lein et al., 2008; Albus et al., 2010; Arsova et al., 2010). Here, we have characterized another of these unknown proteins in detail. Due to its chlorotic phenotype, we called this antisense transformant *LCAA*. The *LCAA* protein is imported into chloroplasts, as supported by in silico predictions for plastid-targeted transit peptides and by the analysis of GFP fusion proteins (Fig. 3). Additionally,

orthologs of *LCAA* were retained in the chloroplast genome in several algal species (Fig. 2).

The *LCAA* antisense plants are characterized by their reduced chlorophyll contents per leaf area and strongly increased chlorophyll *a/b* ratios (Table I). This indicates that mainly the accumulation of the LHC proteins is compromised. Immunoblots confirmed the LHC deficiency (Fig. 4B). On a leaf area basis, the abundance of the photosystems is also clearly reduced in the strong antisense lines. However, the LHC repression is much more pronounced (Table II; Fig. 4A). Because the contents of the cytochrome *b₆f* complex, plastocyanin, and the ATP synthase are less affected (Table II; Fig. 4A), the capacity of photosynthetic electron transport and the maximum quantum efficiency of PSII are very similar in the wild type and all *LCAA* antisense plants. Also, respiration is unaltered (Table I). However, the quantum efficiency of CO_2 fixation is increasingly reduced in the *LCAA* antisense lines, which cannot be exclusively explained by a reduced leaf absorbance due to reduced total chlorophyll content (Table I). Rather, our data indicate an imbalanced excitation of both photosystems, as shown by the more rapid reduction of the plastoquinone pool and the PSII acceptor side in the lines with stronger phenotypes (Fig. 5B). This is well in line with the stronger reduction in PSI than in PSII contents per leaf area (Table II) and with the 77K chlorophyll *a* fluorescence emission spectra (Fig. 5A), which also indicate a reduced total PSI antenna cross-section relative to PSII. Due to the severe reduction in the quantum efficiency of CO_2 fixation, in the strongest antisense line *LCAA4*, leaf assimilation rate at the growth light intensity of $250 \mu\text{E m}^{-2} \text{s}^{-1}$ was reduced to less than 40% of the rate observed in the wild type (Table I). This explains the severe growth retardation of the antisense lines.

Phylogenetic Considerations Suggest a Role of *LCAA* in Chlorophyll Biosynthesis

At first glance, the physiological phenotypes of *LCAA* antisense plants bear close resemblance to mutants impaired in LHC biogenesis or thylakoid membrane insertion via the cpSRP-cpFtsY-Albino3-dependent pathway (Klimyuk et al., 1999; Hutin et al., 2002) as well as to mutants with impaired synthesis of total chlorophyll or, more specifically, chlorophyll *b*. Effects of reduced chlorophyll synthesis on the accumulation of the photosynthetic complexes were first analyzed in plants grown under intermittent light conditions, when the light-dependent step of chlorophyll synthesis catalyzed by POR becomes strongly rate limiting for chlorophyll synthesis. Intermittent-light-grown plants are largely devoid of LHC proteins, as LHC apoproteins are unstable in the thylakoid membranes and rapidly degraded (Cuming and Bennett, 1981). The photosynthetic electron transport chain functions normally in these plants (Jahns and Junge, 1992). Similar phenotypes were also observed in several mutants with reduced rates of chlorophyll synthesis

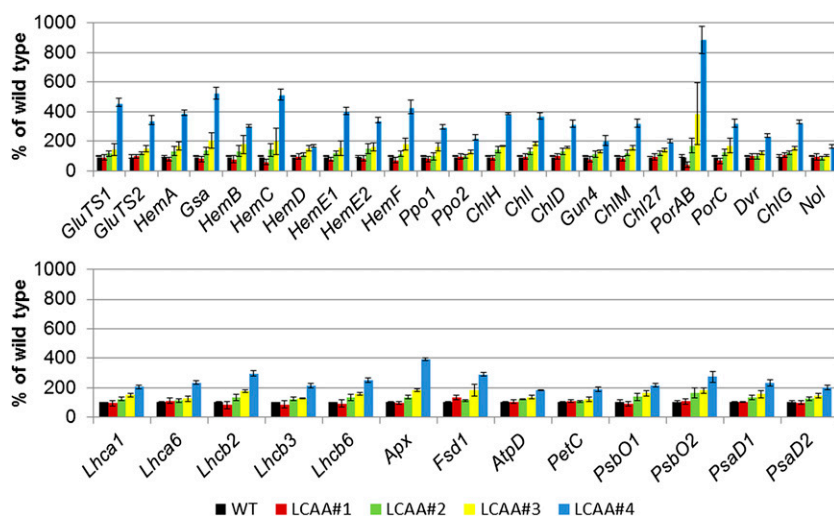


Figure 7. qPCR analyses to quantify transcript accumulation levels of genes involved in tetrapyrrole biosynthesis, photosynthetic light reactions, and the antioxidative system of chloroplasts. Detailed information on primer design and on the closest Arabidopsis homologs of the analyzed genes is provided in Supplemental Table S1. The top panel shows genes involved in tetrapyrrole biosynthesis displayed in the sequence of the chlorophyll biosynthesis pathway. The bottom panel shows genes for light-harvesting complex proteins, photosynthetic complex subunits, and antioxidative enzymes in the chloroplast. WT, Wild type.

(Falbel and Staehelin, 1994; Falbel et al., 1996; Tottey et al., 2003): chlorophyllide *a* oxygenase, which catalyzes the highly regulated step of chlorophyll(ide) *a*-to-chlorophyll(ide) *b* conversion, has a relatively low affinity for chlorophyll(ide) *a*. In consequence, chlorophyll *b* synthesis becomes more active when chlorophyll *a*-binding sites of the reaction center proteins are saturated. For this reason, a modest restriction in chlorophyll synthesis primarily affects LHC accumulation, while strong restrictions also impair the accumulation of other photosynthetic complexes (Hansson and Jensen, 2009; Kim et al., 2009; Dall’Osto et al., 2010).

As the phenotypes observed for the *LCAA* antisense lines are compatible with both a role of *LCAA* in LHC biogenesis and a role in chlorophyll synthesis, which could either be a general one or one specifically affecting the interconversion of chlorophyll(ide) *a* to chlorophyll *b*, we had to distinguish between these scenarios. The phylogenetic distribution of *LCAA* already strongly argues in favor of a role in general chlorophyll synthesis: apart from green algae, mosses, and higher plants, *LCAA* is highly conserved in most cyanobacteria and in rhodophyta, which do not have LHC antenna proteins. However, six *Prochlorococcus* species adapted to low-light environments do not contain an *LCAA* homolog (Castruita et al., 2011).

Circumstantial evidence for a role of *LCAA* in chlorophyll synthesis instead of LHC apoprotein biogenesis also comes from our finding that not all LHC proteins were affected to the same extent (Fig. 4B), which is similar to LHC accumulation defects described in mutants with general reductions in the Mg branch of tetrapyrrole biosynthesis or diminished chlorophyll *b* synthesis capacity (Tanaka and Tanaka, 2011). On the other hand, mutants with reduced availability of chlorophyll due to the antisense repression of *GSAT* display a simultaneous reduction of PSII and PSI reaction centers and their antenna complexes, so that the chlorophyll *a/b* ratio remains constant, despite strong reductions in chlorophyll accumulation (Härtel et al., 1997). As, in contrast, the *LCAA* antisense plants show a gradually reduced

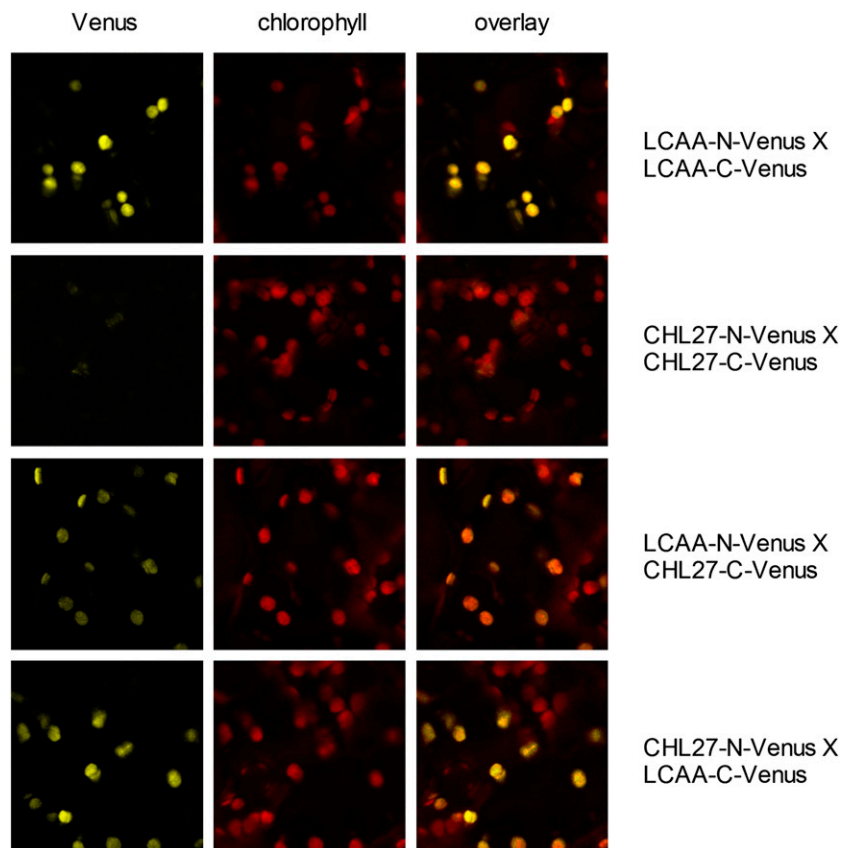
chlorophyll accumulation with an increasing chlorophyll *a/b* ratio and a drastic reduction in the LHC protein content, this might point to a function of *LCAA* in one of the later steps of chlorophyll biosynthesis. To unequivocally assign *LCAA* function to one of the later steps of chlorophyll biosynthesis, we directly measured chlorophyll synthesis rates and the accumulation levels of different intermediates of chlorophyll biosynthesis.

***LCAA* Is Required for the MgProtoMME Cyclase Reaction**

Determination of chlorophyll biosynthesis intermediates suggests that the primary defect caused by *LCAA* deficiency is an impairment of the cyclase reaction, as indicated by the accumulation of MgProtoMME and reduced levels of Pchlde both after ALA feeding (Table III) and under steady-state conditions (Table IV). This resembles Arabidopsis and tobacco mutants deficient in the *CHL27* subunit of the cyclase (Tottey et al., 2003; Peter et al., 2010), which also show a pale-green phenotype. Due to the resemblance of *CHL27*- and *LCAA*-deficient plants, we determined if the accumulation of *CHL27* is compromised in *LCAA* antisense lines. While most other enzymes of tetrapyrrole biosynthesis accumulated normally or even to higher levels than in the wild type, the accumulation of the *CHL27* protein was specifically decreased in the *LCAA* antisense plants (Fig. 6B; see below). Because the specific loss of *CHL27* could not be attributed to a repression of *Chl27* mRNA accumulation (Fig. 7A), we assumed that *LCAA* is essential for the stable accumulation of *CHL27* and the cyclase protein complex. Indeed, bimolecular fluorescence complementation assays (Fig. 8) support a physical interaction between *LCAA* and *CHL27*. Interestingly, in addition to interaction with *CHL27*, *LCAA* also seems to interact with itself, forming homodimers or even oligomers.

These observations are well in line with a recent analysis of *Synechocystis* sp. PCC 6803 knockdown mutants of the cyanobacterial *LCAA* homolog, *ycf54*, which was published while this paper was in revision (Hollingshead et al., 2012). Inactivation of *ycf54* via

Figure 8. Bimolecular fluorescence complementation was applied to analyze the protein-protein interaction of LCAA and CHL27 in chloroplasts. The left column shows restored Venus fluorescence resulting from the interaction of candidate proteins. The middle column shows chlorophyll fluorescence representing chloroplasts. The right column shows merged images demonstrating the colocalization of restored Venus fluorescence and chlorophyll fluorescence. These results show the interaction of LCAA with CHL27 and the homodimerization of LCAA. However, no homodimerization of CHL27 was detected.



gene disruption with an erythromycin resistance cassette resulted in chlorophyll deficiency and high accumulation levels of MgProtoMME, similar to our results in higher plants. Also, loss of the major homolog of CHL27 in *Synechocystis* sp. PCC 6803, Sll1214, was observed. Ycf54 in *Synechocystis* sp. PCC 6803 localizes both to the thylakoid membrane and in the stroma. For LCAA, such a distribution is tentatively supported by our experiments showing an equal distribution of LCAA-GFP throughout the chloroplast (Fig. 3). Therefore, the function of *LCAA/ycf54* seems to be highly conserved from cyanobacteria to higher plants.

Deficiency of LCAA Affects ALA Synthesis and the Accumulation of Proteins in Tetrapyrrole Biosynthesis

LCAA down-regulation not only compromises the accumulation of CHL27 and the catalytic formation of Pchlide, as indicated by accumulated MgProtoMME and reduced steady-state levels of Pchlide (Table IV) and chlorophyll (Table I), it also affects the accumulation of several other proteins of tetrapyrrole metabolism (Fig. 6B), which turned out to be more abundant upon reduced *LCAA* expression. In particular, an increased abundance of GluTR, CHLH, and POR was observed. These proteins are positioned at important regulatory steps of the tetrapyrrole metabolism. GluTR is the initial enzyme of the pathway, the CHLH subunit of Mg chelatase is at the branch point for the

allocation of protoporphyrin IX to heme or chlorophyll biosynthesis, and POR is the enzyme for the light-dependent reduction of Pchlide in dicotyledonous plants. The increased GluTR levels coincide with increased ALA synthesis rates (Fig. 6A), suggesting that reduced *LCAA* expression could stimulate ALA synthesis through a defective feedback-control mechanism. This increased protein accumulation correlates well with increased transcript amounts of all tested enzymes of tetrapyrrole biosynthesis (Fig. 7). However, the correlation between transcript abundance, protein accumulation, and the severity of the antisense phenotype is discontinued from antisense line 3 to line 4. This could be due to secondary effects of the strong reduction in chlorophyll content and the quantum efficiency of CO₂ fixation in antisense line *LCAA4*. The severe repression of the quantum efficiency of CO₂ fixation in antisense line *LCAA4* results in a more than 60% reduction in leaf assimilation at the growth light intensity relative to the wild type. As a consequence, a general bioenergetic limitation of growth and protein biosynthesis may occur. The general up-regulation of photosynthetic gene expression in the nucleus could be due to the absence of negative signals arising from high photoassimilate accumulation in mature source leaves of wild-type tobacco (sugar sensing; for review, see Koch, 1996; Pego et al., 2000). However, the severe reduction in the quantum efficiency of CO₂ fixation especially in antisense line *LCAA4* might already bioenergetically limit

the capacity of the transformants for protein biosynthesis, thereby resulting in decreased protein accumulation levels, in spite of increased transcript abundances for the enzymes of tetrapyrrole biosynthesis. A similar reduction in POR accumulation to that observed in the strong *LCAA4* antisense line was also reported for the $\Delta ycf54$ mutant of *Synechocystis* sp. PCC 6803 (Hollingshead et al., 2012). Our data suggest that this loss of POR might also be an indirect effect of decreased photosynthetic activity, which is not specifically attributable to a function of LCAA in POR accumulation.

Potential Roles of LCAA

Based on our observations, two major roles of LCAA are suggested. (1) LCAA is an essential component of a functional cyclase and ensures chlorophyll biosynthesis. While CHL27 resembles the catalytic subunit of monooxygenase-related proteins, which also consist of a reducing subunit and a scaffold subunit (Berthold and Stenmark, 2003), no structural similarity of LCAA to a reductase is apparent. Therefore, it is proposed that LCAA functions as a scaffold protein that tethers the cyclase reaction to other proteins of the pathway, its regulators, or metabolites. Because of its tentative suborganellar localization in both thylakoid membrane and stroma, LCAA could represent either the second membrane-associated component or the soluble component of the cyclase system. However, in the barley *viridis-k* mutant deficient in the second membrane-associated cyclase subunit, accumulation of CHL27 was unaltered or even increased (Rzeznicka et al., 2005), strongly arguing against LCAA being this second membrane-associated cyclase subunit. The molecular mass of the soluble cyclase component was suggested to be larger than 30 kD (Walker et al., 1991); while this is larger than the LCAA monomer, the homooligomerization of LCAA suggested by our bimolecular fluorescence complementation analysis might explain the size difference between the suggested soluble cyclase component and LCAA. Alternatively, LCAA could be a fourth protein of the cyclase complex, for which neither biochemical nor genetic evidence has been obtained in previous studies. (2) In addition to its role in the cyclase reaction, LCAA connects the cyclase activity with ALA synthesis. Comparing the physiological impact of inactivated expression of the two putative subunits of the cyclase, *LCAA* silencing in tobacco causes a different response of enzymes of tetrapyrrole biosynthesis than CHL27 deficiency in transgenic tobacco plants, even though the visible phenotypes are very similar. CHL27 antisense plants do not show elevated levels of ALA biosynthesis and do not accumulate GluTR and CHLH (Peter et al., 2010). As both sets of transformants contain reduced CHL27 protein levels, the different effects on tetrapyrrole biosynthesis in *LCAA* antisense plants must be due to deficient *LCAA* expression resulting in either a feedback-controlled stimulation or a release of the suppression of ALA synthesis.

Future work will explore the potential interactions of LCAA with other proteins of chlorophyll biosynthesis and will investigate the assembly of chlorophyll into the photosynthetic chlorophyll-binding proteins. A functional interplay of the aerobic cyclase with other components of chlorophyll synthesis could ensure the integrity of chlorophyll metabolism and facilitate the efficient assembly of chlorophyll into chlorophyll-binding proteins.

MATERIALS AND METHODS

Plant Material and Growth Conditions

Construction of the tobacco (*Nicotiana tabacum*) *LCAA* antisense vector and phenotyping of transgenic plants was performed as described by Lein et al. (2008). The antisense construct covering 21 bp of the 5' untranslated region, the complete coding region, and 329 bp of the 3' untranslated region of *LCAA* was expressed under the control of the cauliflower mosaic virus 35S promoter and assembled in a plasmid vector as described. Correct insertion of the cassette was verified by PCR with genomic DNA as template and primers P35S (5'-GTGGATTGATGTGATATCTCC-3') and POCS (5'-GTAAGGATCTGAGCTACACAT-3') followed by direct sequencing of the PCR products (Lein et al., 2008). Tobacco transformation by *Agrobacterium tumefaciens*-mediated gene transfer using *A. tumefaciens* strain C58C1:pGV2260 was carried out as described (Rosahl et al., 1987). For all experiments, plants were raised from seeds germinated on petri dishes containing Murashige and Skoog medium supplemented with 2% (w/v) Suc and 300 $\mu\text{g mL}^{-1}$ kanamycin. Wild-type seedlings were grown on the medium without kanamycin. Fourteen days after germination, the seedlings were transferred to a soil:vermiculite mixture (2:1; Florargard Vertriebs GmbH) and grown in a controlled-environment chamber at 120 $\mu\text{E m}^{-2} \text{s}^{-1}$ light intensity, 22°C, and 75% relative humidity under long-day conditions (16 h of light). In the night, the temperature was reduced to 18°C. After another 2 weeks, plants were transferred to the greenhouse. Light intensity at the level of the youngest leaves was approximately 250 $\mu\text{E m}^{-2} \text{s}^{-1}$.

Northern-Blot Analysis

RNA was extracted from leaves using the peqGold Trifast reagent (Peqlab). Samples equivalent to 2.5 μg of RNA were separated on 1% formaldehyde-containing agarose gels and blotted onto Hybond-XL nylon membranes. An *LCAA*-specific probe was generated by PCR amplification from tobacco cDNA with the primers *LCAA*fw (5'-GCTGTTGATTCCTCTGAGCCT-3') and *LCAA*rv (5'-GGAGTACATGCCAAAGCTTC-3'). For hybridization, [α - ^{32}P] dCTP-labeled probes were generated by random priming (Multiprime DNA labeling kit; GE Healthcare). Hybridizations were carried out at 65°C in Rapid Hybridization Buffer (GE Healthcare) following the manufacturer's protocol. Hybridization signals were detected by x-ray film exposure.

qPCR Primer Design and Test

Annotated protein sequences of Arabidopsis (*Arabidopsis thaliana*) were used to search against the translated EST database of tobacco using the National Center for Biotechnology Information Web page (<http://blast.ncbi.nlm.nih.gov/Blast.cgi>). The identified ESTs were assembled using the SeqMan Pro software (DNASTAR). To facilitate qPCR measurements, primers were derived from sequences close to the 3' end of the coding regions using QuantPrime (Arvidsson et al., 2008) and the following parameters: melting temperature of 60°C, amplicon length between 50 and 150 bp, and GC content of 35% to 65%. The PCR specificity was confirmed by a melting-curve analysis after 45 amplification cycles (LightCycler 480 Real-Time PCR System; Roche Diagnostics) and by gel electrophoresis.

Real-Time Quantitative Reverse Transcription-PCR

For real-time quantitative reverse transcription-PCR analysis, total RNA was extracted using the NucleoSpin RNA Plant Kit (Macherey-Nagel). The eluted RNA was digested with TURBO DNase (Life Technologies). To test for

the absence of DNA contaminations, an aliquot of the RNA sample was used as template in a PCR using primers (forward, 5'-ACGGGTCAATCTT-CAACCAG-3'; reverse, 5'-CAGAAAGCGTTTGATCAGCA-3') targeting the tobacco vacuolar invertase gene (AJ305044). All RNA samples were tested alongside a positive control using genomic DNA of tobacco. After the absence of DNA contaminations was confirmed, RNA integrity was checked on a 1% denaturing agarose gel. One microgram of total RNA was subsequently used for cDNA synthesis with SuperScriptIII reverse transcriptase (Life Technologies) according to the manufacturer's instructions. Quantitative reverse transcription-PCR was performed on optical 384-well plates with a Light-Cycler 480 Real-Time PCR System (Roche Diagnostics). The reactions contained 2.5 μ L of LightCycler 480 SYBR Green I Master (Roche Diagnostics), 500 nm of each gene-specific primer, and 0.5 μ L of cDNA in a 1:100 dilution, resulting in a total reaction volume of 5 μ L. The following thermal profile was used for all PCR reactions: 95°C for 10 min, 45 cycles of 95°C, 60°C, and 72°C for 10 s at each temperature step. The melting curve was recorded after cycle 45 by heating from 65°C to 95°C with a ramp speed of 0.11°C s⁻¹. The LightCycler 480 Software (Roche Diagnostics) was used for data analysis. The cycle in which the fluorescence of a sample exceeded the background, called the "crossing point," was calculated using the second derivative maximum method. For each primer pair, a standard curve was run in parallel to the analyzed samples. Each standard curve consisted of four different dilutions (1:20, 1:100, 1:1,000, 1:10,000) of wild-type cDNA. The relative template input was calculated based on the standard curve for each primer pair. To ensure correct normalization of the investigated genes, we tested the expression of 10 different genes suggested for use as reference genes in Arabidopsis (Czechowski et al., 2005) and tobacco (Schmidt and Delaney, 2010) and ranked them by their expression stability using geNorm (Vandesompele et al., 2002). Three reference genes showing the most stable gene expression in all four LCAA antisense lines and the corresponding wild type were chosen for normalization of our experiments: Actin, a SAND family protein (homologous to AT2G28390), and a clathrin adaptor subunit (homologous to At5g46630). Three technical replicates were measured for each of the four biological replicates analyzed per antisense line.

Bimolecular Fluorescence Complementation Assay

Coding regions of *LCAA* and *Chl27* from Arabidopsis cDNA were both cloned into destination vectors pDEST-GWVYNE (G1) and pDEST-GWVYCE (G3) (Gehl et al., 2009). Constructs were transiently cotransformed into *Nicotiana benthamiana* leaves with *A. tumefaciens* GV2260 at an optical density of 0.2 for each strain. Plants were kept for 2 d in dark before analysis of infected leaf discs by confocal microscopy (excitation at 514 nm wavelength, emission of Venus at 525–600 nm, emission of chlorophyll at 620–700 nm).

Gas-Exchange Measurements

Leaf assimilation was measured on intact tobacco plants using the GFS-3000FL gas-exchange system equipped with the standard measuring head 3010-S (8-cm² leaf area) and the LED-Array/PAM-fluorometer module 3055-FL for actinic illumination and chlorophyll *a* fluorescence determination (Heinz Walz). Light-response curves of CO₂ fixation were measured at 20°C cuvette temperature, 17,500 μ L L⁻¹ humidity, in 2,000 μ L L⁻¹ CO₂. The light intensity was stepwise increased from 0 to 2,000 μ E m⁻² s⁻¹. At each light intensity, gas exchange was recorded until a steady state of assimilation and transpiration was achieved. The quantum efficiency of CO₂ fixation was determined in the linear light-response range between 0 and 80 μ E m⁻² s⁻¹. After the end of the gas-exchange measurements, leaf absorbance was determined using an integrating sphere (ISV-469; Jasco) attached to the V550 spectrophotometer (Jasco). The spectral bandwidth was set to 1 nm, and the scanning speed was 200 nm min⁻¹. Transmission and reflectance spectra were measured between 700 and 400 nm wavelength, and leaf absorbance was calculated as 100% – transmittance (%) – reflectance (%). Finally, the chlorophyll content of the measured leaf discs was determined according to Porra et al. (1989) in 80% (v/v) acetone.

Thylakoid Membrane Isolation and Quantitation of Photosynthetic Complexes

Thylakoid membranes were isolated according to Schöttler et al. (2004). The contents of PSII and cytochrome *b₆f* were determined from difference absorbance signals of cytochrome *b₅₅₉* (PSII) and cytochrome *f* and *b₆*. Thylakoids equivalent to 50 μ g chlorophyll mL⁻¹ were destacked in a low-salt medium to

improve the optical properties of the probe (Kirchhoff et al., 2002). All cytochromes were oxidized by the addition of 1 mM potassium ferricyanide (+III) and subsequently reduced by the addition of 10 mM sodium ascorbate and dithionite, resulting in the reduction of cytochrome *f* and the high-potential form of cytochrome *b₅₅₉* (ascorbate-ferricyanide difference spectrum) and of cytochrome *b₆* and the low-potential form of cytochrome *b₅₅₉*, respectively. At each redox potential, absorption spectra were measured between 575 and 540 nm wavelength with a V-550 spectrophotometer (Jasco) equipped with a head-on photomultiplier. The spectral bandwidth was 1 nm, and the scanning speed was 100 nm min⁻¹. Difference absorption spectra were deconvoluted using reference spectra and difference extinction coefficients as described by Kirchhoff et al. (2002). PSII contents were calculated from the sum of the high- and low-potential difference absorption signals of cytochrome *b₅₅₉* (Lamkemeyer et al., 2006). The content of redox-active PSI was determined from light-induced difference absorption changes of P₇₀₀, the PSI reaction center chlorophyll *a* dimer. Thylakoids equivalent to 50 μ g chlorophyll mL⁻¹ were solubilized with 0.2% (w/v) β -dodecyl maltoside in the presence of 100 μ M paraquat as electron acceptor and 10 mM sodium ascorbate as electron donor. P₇₀₀ was oxidized by the application of a saturating light pulse (2,000 μ E m⁻² s⁻¹ red light, 200-ms duration). Measurements were done using the Dual-PAM instrument (Heinz Walz) in its Plastocyanin-P₇₀₀ version (see below). Plastocyanin contents, relative to P₇₀₀, were determined by in vivo difference absorption spectroscopy in the far-red range of the spectrum and then recalculated based on the absolute P₇₀₀ quantification in isolated thylakoids. Light-induced absorption changes at 800 to 870 nm wavelength (where the contribution of P₇₀₀ is predominant) and at 870 to 950 nm wavelength (predominantly arising from plastocyanin) were measured on preilluminated leaves with fully activated Calvin cycle, to avoid acceptor side limitation of PSI (Schöttler et al., 2007).

Chlorophyll *a* Fluorescence

77K chlorophyll *a* fluorescence emission was determined on freshly isolated thylakoids equivalent to 10 μ g chlorophyll mL⁻¹ using a F-6500 fluorometer (Jasco). The sample was excited at 430 nm wavelength (10 nm bandwidth). The emission spectra between 655 and 800 nm were recorded with a bandwidth of 1 nm. Chlorophyll *a* fluorescence of intact leaves was measured at room temperature using a Dual-PAM-100 instrument (Heinz Walz). Light-response curves of nonphotochemical quenching, and the redox state of the PSII acceptor side were recorded on intact leaves after 30 min of dark adaptation. The redox state of the PSII acceptor side was calculated from the qL parameter (Kramer et al., 2004), while qN was determined according to Krause and Weis (1991).

Protein Gel Electrophoresis and Immunoblotting

Thylakoid proteins separated by SDS-PAGE (Perfect Blue twin gel system; Peqlab) were transferred to a polyvinylidene difluoride membrane (Hybond P) using a tank blotting system (Perfect Blue Web M; Peqlab). Immunobiochemical detection was carried out with the enhanced chemiluminescence system (GE Healthcare) according to the instructions of the manufacturer. All antibodies against components of the photosynthetic apparatus were purchased from Agrisera. To analyze proteins involved in tetrapyrrole synthesis, leaf samples were ground in liquid nitrogen and proteins were extracted in 500 μ L of extraction buffer (2% [w/v] SDS, 56 mM Na₂CO₃, 12% [w/v] Suc, 56 mM dithiothreitol, and 1 mM EDTA, pH 8.0) for 10 min at 75°C and centrifuged. The protein concentration was determined with the bicinchoninic acid reagent (Thermo Scientific). Soluble proteins were separated on 8% or 12% polyacrylamide gels, transferred to Hybond-C membranes (GE Healthcare), and probed with antibodies raised against enzymes of tetrapyrrole biosynthesis. Antibodies against GluTR, GSAT, CHLM were made in the Grimm laboratory. Anti-pea (*Pisum sativum*) CHLD and CHLH antibodies were kindly provided by Prof. M. Luo (Huazhong Agricultural University); anti-NTRC and anti-LIL3 antibodies were kindly provided by Prof. E. Rintamaki (University of Turku) and Prof. R. Tanaka (Hokkaido University), respectively. Anti-CHL27 and POR were purchased from Agrisera.

Analysis of ALA-Synthesizing Capacity

The rate of ALA synthesis was measured according to Mauzerall and Granick (1956), and experiments with leaf samples were performed according

to protocols described previously (Papenbrock et al., 1999; Shalygo et al., 2009).

ALA Feeding Experiments

Tobacco leaf discs were incubated in 1 mM ALA (50 mM HEPES, pH 7.5). The incubation was carried out under continuous white light ($30 \mu\text{E m}^{-2} \text{s}^{-1}$) at 22°C for 24 h. Subsequently, leaf discs were dried, weighed, and frozen in liquid nitrogen.

Determination of Mg Porphyrins and Pchl_a Contents

Porphyrins were extracted in acetone:methanol:0.1 N NH₄OH (10:9:1, v/v/v) and analyzed via HPLC as described by Papenbrock et al. (1999). For Pchl_a extraction, leaf samples were weighted, frozen, ground in liquid nitrogen, and extracted twice in alkaline acetone (9:1 100% acetone:0.1 N NH₄OH). Aliquots of the supernatants were applied to the Agilent HPLC System 1290 and separated by a reverse-phase column (Waters WAT036975, Nova-Pak C18; 4 μm , 150 \times 3.9 mm, flow rate of 1.0 mL min⁻¹) using solvents A (20% 1 M ammonium acetate, pH 7.0, 80% methanol [v/v]) and B (20% acetone, 80% methanol [v/v]) with the following program: 9-min linear gradient from 100% A to 60% A/40% B, continued for 6 min with 100% B, then returned to 100% A within 1 min, followed by an additional 6 min with solvent A. Fluorescence detection and Pchl_a quantification were performed according to Richter et al. (2010a).

Supplemental Data

The following materials are available in the online version of this article.

Supplemental Table S1. Overview of forward (F) and reverse (R) primers used for the qPCR analyses shown in Figure 7.

ACKNOWLEDGMENTS

We thank Sabeeha Merchant (University of California, Los Angeles) for stimulating discussions. We are grateful to Britta Hausmann and Helga Kulka (Max-Planck-Institut für Molekulare Pflanzenphysiologie) for plant cultivation.

Received August 23, 2012; accepted October 18, 2012; published October 19, 2012.

LITERATURE CITED

- Albus CA, Ruf S, Schöttler MA, Lein W, Kehr J, Bock R (2010) Y3IP1, a nucleus-encoded thylakoid protein, cooperates with the plastid-encoded Ycf3 protein in photosystem I assembly of tobacco and *Arabidopsis*. *Plant Cell* **22**: 2838–2855
- Andersson J, Wentworth M, Walters RG, Howard CA, Ruban AV, Horton P, Jansson S (2003) Absence of the Lhcb1 and Lhcb2 proteins of the light-harvesting complex of photosystem II: effects on photosynthesis, grana stacking and fitness. *Plant J* **35**: 350–361
- Arsova B, Hoja U, Wimmelbacher M, Greiner E, Ustün S, Melzer M, Petersen K, Lein W, Börnke F (2010) Plastidial thioredoxin z interacts with two fructokinase-like proteins in a thiol-dependent manner: evidence for an essential role in chloroplast development in *Arabidopsis* and *Nicotiana benthamiana*. *Plant Cell* **22**: 1498–1515
- Arvidsson S, Kwasniewski M, Riaño-Pachón DM, Mueller-Roeber B (2008) QuantPrime: a flexible tool for reliable high-throughput primer design for quantitative PCR. *BMC Bioinformatics* **9**: 465
- Bannai H, Tamada Y, Maruyama O, Nakai K, Miyano S (2002) Extensive feature detection of N-terminal protein sorting signals. *Bioinformatics* **18**: 298–305
- Bellemare G, Bartlett SG, Chua NH (1982) Biosynthesis of chlorophyll a/b-binding polypeptides in wild type and the chlorina f2 mutant of barley. *J Biol Chem* **257**: 7762–7767
- Berthold DA, Stenmark P (2003) Membrane-bound diiron carboxylate proteins. *Annu Rev Plant Biol* **54**: 497–517
- Bossmann B, Knoetzel J, Jansson S (1997) Screening of chlorina mutants of barley (*Hordeum vulgare* L.) with antibodies against light-harvesting proteins of PS I and PS II: absence of specific antenna proteins. *Photosynth Res* **52**: 127–136
- Castroita M, Casero D, Karpowicz SJ, Kropat J, Vieler A, Hsieh SI, Yan W, Cokus S, Loo JA, Benning C, et al (2011) Systems biology approach in *Chlamydomonas* reveals connections between copper nutrition and multiple metabolic steps. *Plant Cell* **23**: 1273–1292
- Cuming AC, Bennett J (1981) Biosynthesis of the light-harvesting chlorophyll a/b protein: control of messenger RNA activity by light. *Eur J Biochem* **118**: 71–80
- Czarnecki O, Grimm B (2012) Post-translational control of tetrapyrrole biosynthesis in plants, algae, and cyanobacteria. *J Exp Bot* **63**: 1675–1687
- Czechowski T, Stitt M, Altmann T, Udvardi MK, Scheible WR (2005) Genome-wide identification and testing of superior reference genes for transcript normalization in *Arabidopsis*. *Plant Physiol* **139**: 5–17
- Dall’Osto L, Cazzaniga S, Havaux M, Bassi R (2010) Enhanced photoprotection by protein-bound vs free xanthophyll pools: a comparative analysis of chlorophyll b and xanthophyll biosynthesis mutants. *Mol Plant* **3**: 576–593
- DellaPenna D, Pogson BJ (2006) Vitamin synthesis in plants: tocopherols and carotenoids. *Annu Rev Plant Biol* **57**: 711–738
- Eberhard S, Finazzi G, Wollman FA (2008) The dynamics of photosynthesis. *Annu Rev Genet* **42**: 463–515
- Emanuelsson O, Brunak S, von Heijne G, Nielsen H (2007) Locating proteins in the cell using TargetP, SignalP and related tools. *Nat Protoc* **2**: 953–971
- Engelken J, Brinkmann H, Adamska I (2010) Taxonomic distribution and origins of the extended LHC (light-harvesting complex) antenna protein superfamily. *BMC Evol Biol* **10**: 233
- Falbel TG, Meehl JB, Staehelin LA (1996) Severity of mutant phenotype in a series of chlorophyll-deficient wheat mutants depends on light intensity and the severity of the block in chlorophyll synthesis. *Plant Physiol* **112**: 821–832
- Falbel TG, Staehelin LA (1994) Characterization of a family of chlorophyll-deficient wheat (*Triticum*) and barley (*Hordeum vulgare*) mutants with defects in the magnesium-insertion step of chlorophyll biosynthesis. *Plant Physiol* **104**: 639–648
- Felder S, Meierhoff K, Sane AP, Meurer J, Driemel C, Plücken H, Klaff P, Stein B, Bechtold N, Westhoff P (2001) The nucleus-encoded *HCF107* gene of *Arabidopsis* provides a link between intercistronic RNA processing and the accumulation of translation-competent *psbH* transcripts in chloroplasts. *Plant Cell* **13**: 2127–2141
- Ferro M, Brugière S, Salvi D, Seigneurin-Berny D, Court M, Moyet L, Ramus C, Miras S, Mellal M, Le Gall S, et al (2010) AT_CHLORO, a comprehensive chloroplast proteome database with subplastidial localization and curated information on envelope proteins. *Mol Cell Proteomics* **9**: 1063–1084
- Ganeteg U, Strand A, Gustafsson P, Jansson S (2001) The properties of the chlorophyll a/b-binding proteins Lhca2 and Lhca3 studied in vivo using antisense inhibition. *Plant Physiol* **127**: 150–158
- Gehl C, Waadt R, Kudla J, Mendel RR, Hänsch R (2009) New Gateway vectors for high throughput analyses of protein-protein interactions by bimolecular fluorescence complementation. *Mol Plant* **2**: 1051–1058
- Gough S (1972) Defective synthesis of porphyrins in barley plastids caused by mutation in nuclear genes. *Biochim Biophys Acta* **286**: 36–54
- Grimm B (2010) Control of the metabolic flow in tetrapyrrole biosynthesis: regulation of expression and activity of enzymes in the Mg branch of tetrapyrrole biosynthesis. In CA Rebeiz, C Benning, HJ Bohnert, H Daniel, K Hooper, HK Lichtenthaler, AR Portis, BC Tripathy, eds, *The Chloroplast*. Springer, Dordrecht, The Netherlands, pp 39–53
- Hansson A, Jensen PE (2009) Chlorophyll limitation in plants remodels and balances the photosynthetic apparatus by changing the accumulation of photosystems I and II through two different approaches. *Physiol Plant* **135**: 214–228
- Härtel H, Kruse E, Grimm B (1997) Restriction of chlorophyll synthesis due to expression of glutamate-1-semialdehyde aminotransferase antisense RNA does not reduce the light-harvesting antenna size in tobacco. *Plant Physiol* **113**: 1113–1124
- Havaux M, Dall’Osto L, Bassi R (2007) Zeaxanthin has enhanced antioxidant capacity with respect to all other xanthophylls in *Arabidopsis* leaves and functions independent of binding to PSII antennae. *Plant Physiol* **145**: 1506–1520

- Hollingshead S, Kopečná J, Jackson PJ, Canniffe DP, Davison PA, Dickman MJ, Sobotka R, Hunter CN (2012) Conserved chloroplast open-reading frame ycf54 is required for activity of the magnesium protoporphyrin monomethylester oxidative cyclase in *Synechocystis* PCC 6803. *J Biol Chem* **287**: 27823–27833
- Horn R, Grundmann G, Paulsen H (2007) Consecutive binding of chlorophylls a and b during the assembly in vitro of light-harvesting chlorophyll-a/b protein (LHCIIb). *J Mol Biol* **366**: 1045–1054
- Hutin C, Havaux M, Carde JP, Kloppstech K, Meierhoff K, Hoffman N, Nussaume L (2002) Double mutation cpSRP43–/cpSRP54– is necessary to abolish the cpSRP pathway required for thylakoid targeting of the light-harvesting chlorophyll proteins. *Plant J* **29**: 531–543
- Jahns P, Junge W (1992) Thylakoids from pea seedlings grown under intermittent light: biochemical and flash-spectrophotometric properties. *Biochemistry* **31**: 7390–7397
- Jansson S (1999) A guide to the Lhc genes and their relatives in *Arabidopsis*. *Trends Plant Sci* **4**: 236–240
- Karpowicz SJ, Prochnik SE, Grossman AR, Merchant SS (2011) The GreenCut2 resource, a phylogenetically derived inventory of proteins specific to the plant lineage. *J Biol Chem* **286**: 21427–21439
- Kim EH, Li XP, Razeghifard R, Anderson JM, Niyogi KK, Pogson BJ, Chow WS (2009) The multiple roles of light-harvesting chlorophyll a/b-protein complexes define structure and optimize function of *Arabidopsis* chloroplasts: a study using two chlorophyll b-less mutants. *Biochim Biophys Acta* **1787**: 973–984
- Kirchhoff H, Mukherjee U, Galla HJ (2002) Molecular architecture of the thylakoid membrane: lipid diffusion space for plastoquinone. *Biochemistry* **41**: 4872–4882
- Kleine T, Maier UG, Leister D (2009) DNA transfer from organelles to the nucleus: the idiosyncratic genetics of endosymbiosis. *Annu Rev Plant Biol* **60**: 115–138
- Klimyuk VI, Persello-Cartiaux F, Havaux M, Contard P, Schuenemann D, Meierhoff K, Gouet P, Jones JDG, Hoffman NE, Nussaume L (1999) A chromodomain protein encoded by the *Arabidopsis* CAO gene is a plant-specific component of the chloroplast signal recognition particle pathway that is involved in LHCP targeting. *Plant Cell* **11**: 87–99
- Koch KE (1996) Carbohydrate-modulated gene expression in plants. *Annu Rev Plant Physiol Plant Mol Biol* **47**: 509–540
- Kramer DM, Johnson G, Kiirats O, Edwards GE (2004) New fluorescence parameters for the determination of q(a) redox state and excitation energy fluxes. *Photosynth Res* **79**: 209–218
- Krause GH, Weis E (1991) Chlorophyll-a fluorescence and photosynthesis: the basics. *Annu Rev Plant Physiol Plant Mol Biol* **42**: 313–349
- Król M, Spangfort MD, Huner NP, Oquist G, Gustafsson P, Jansson S (1995) Chlorophyll a/b-binding proteins, pigment conversions, and early light-induced proteins in a chlorophyll b-less barley mutant. *Plant Physiol* **107**: 873–883
- Lamkemeyer P, Laxa M, Collin V, Li W, Finkemeier I, Schöttler MA, Holtkamp V, Tognetti VB, Issakidis-Bourguet E, Kandlbinder A, et al (2006) Peroxiredoxin Q of *Arabidopsis thaliana* is attached to the thylakoids and functions in context of photosynthesis. *Plant J* **45**: 968–981
- Lein W, Usadel B, Stitt M, Reindl A, Ehrhardt T, Sonnwald U, Börnke F (2008) Large-scale phenotyping of transgenic tobacco plants (*Nicotiana tabacum*) to identify essential leaf functions. *Plant Biotechnol J* **6**: 246–263
- Lezhneva L, Meurer J (2004) The nuclear factor HCF145 affects chloroplast psaA-psaB-rps14 transcript abundance in *Arabidopsis thaliana*. *Plant J* **38**: 740–753
- Lunn JE (2007) Compartmentation in plant metabolism. *J Exp Bot* **58**: 35–47
- Lyska D, Paradis S, Meierhoff K, Westhoff P (2007) HCF208, a homolog of *Chlamydomonas* CCB2, is required for accumulation of native cytochrome b6 in *Arabidopsis thaliana*. *Plant Cell Physiol* **48**: 1737–1746
- Ma J, Peng L, Guo J, Lu Q, Lu C, Zhang L (2007) LPA2 is required for efficient assembly of photosystem II in *Arabidopsis thaliana*. *Plant Cell* **19**: 1980–1993
- Masuda T (2008) Recent overview of the Mg branch of the tetrapyrrole biosynthesis leading to chlorophylls. *Photosynth Res* **96**: 121–143
- Mauzerall D, Granick S (1956) The occurrence and determination of delta-amino-levulinic acid and porphobilinogen in urine. *J Biol Chem* **219**: 435–446
- Meskauskiene R, Nater M, Goslings D, Kessler F, op den Camp R, Apel K (2001) FLU: a negative regulator of chlorophyll biosynthesis in *Arabidopsis thaliana*. *Proc Natl Acad Sci USA* **98**: 12826–12831
- Meurer J, Meierhoff K, Westhoff P (1996) Isolation of high-chlorophyll-fluorescence mutants of *Arabidopsis thaliana* and their characterisation by spectroscopy, immunoblotting and northern hybridisation. *Planta* **198**: 385–396
- Meurer J, Plücker H, Kowallik KV, Westhoff P (1998) A nuclear-encoded protein of prokaryotic origin is essential for the stability of photosystem II in *Arabidopsis thaliana*. *EMBO J* **17**: 5286–5297
- Minamizaki K, Mizoguchi T, Goto T, Tamiaki H, Fujita Y (2008) Identification of two homologous genes, chlAI and chlAII, that are differentially involved in isocyclic ring formation of chlorophyll a in the cyanobacterium *Synechocystis* sp. PCC 6803. *J Biol Chem* **283**: 2684–2692
- Mochizuki N, Tanaka R, Grimm B, Masuda T, Moulin M, Smith AG, Tanaka A, Terry MJ (2010) The cell biology of tetrapyrroles: a life and death struggle. *Trends Plant Sci* **15**: 488–498
- Moseley JL, Page MD, Alder NP, Eriksson M, Quinn J, Soto F, Theg SM, Hippler M, Merchant S (2002) Reciprocal expression of two candidate di-iron enzymes affecting photosystem I and light-harvesting complex accumulation. *Plant Cell* **14**: 673–688
- Moulin M, Smith AG (2005) Regulation of tetrapyrrole biosynthesis in higher plants. *Biochem Soc Trans* **33**: 737–742
- Noctor G, Foyer CH (1998) A re-evaluation of ATP:NADPH budget during C3 photosynthesis: a contribution from nitrate assimilation and its associated respiratory activity. *J Exp Bot* **49**: 1895–1908
- Papenbrock J, Mock HP, Kruse E, Grimm B (1999) Expression studies in tetrapyrrole biosynthesis: inverse maxima of magnesium chelatase and ferrochelatase. *Planta* **208**: 264–273
- Papenbrock J, Pfündel E, Mock HP, Grimm B (2000) Decreased and increased expression of the subunit CHL I diminishes Mg chelatase activity and reduces chlorophyll synthesis in transgenic tobacco plants. *Plant J* **22**: 155–164
- Pego JV, Kortstee AJ, Huijser C, Smeekens SCM (2000) Photosynthesis, sugars and the regulation of gene expression. *J Exp Bot* **51**: 407–416
- Peng L, Ma J, Chi W, Guo J, Zhu S, Lu Q, Lu C, Zhang L (2006) LOW PSII ACCUMULATION1 is involved in efficient assembly of photosystem II in *Arabidopsis thaliana*. *Plant Cell* **18**: 955–969
- Peter E, Rothbart M, Oelze ML, Shalygo N, Dietz KJ, Grimm B (2010) Mg protoporphyrin monomethylester cyclase deficiency caused photooxidation to different extent in light/dark or continuous light growth. *Plant Cell Physiol* **51**: 1229–1241
- Peter E, Salinas A, Wallner T, Jeske D, Dienst D, Wilde A, Grimm B (2009) Differential requirement of two homologous proteins encoded by sll1214 and sll1874 for the reaction of Mg protoporphyrin monomethylester oxidative cyclase under aerobic and micro-oxic growth conditions. *Biochim Biophys Acta* **1787**: 1458–1467
- Pinta V, Picaud M, Reiss-Husson F, Astier C (2002) Rubrivivax gelatinosus acsF (previously orf358) codes for a conserved, putative binuclear-iron-cluster-containing protein involved in aerobic oxidative cyclization of Mg-protoporphyrin IX monomethylester. *J Bacteriol* **184**: 746–753
- Porra RJ, Thompson WA, Kriedemann PE (1989) Determination of accurate extinction coefficient and simultaneous equations for assaying chlorophylls a and b extracted with four different solvents: verification of the concentration of chlorophyll standards by atomic absorption spectroscopy. *Biochim Biophys Acta* **975**: 384–394
- Richly E, Leister D (2004) An improved prediction of chloroplast proteins reveals diversities and commonalities in the chloroplast proteomes of *Arabidopsis* and rice. *Gene* **329**: 11–16
- Richter A, Peter E, Pörs Y, Lorenzen S, Grimm B, Czarniecki O (2010a) Rapid dark repression of 5-aminolevulinic acid synthesis in green barley leaves. *Plant Cell Physiol* **51**: 670–681
- Richter CV, Bals T, Schünemann D (2010b) Component interactions, regulation and mechanisms of chloroplast signal recognition particle-dependent protein transport. *Eur J Cell Biol* **89**: 965–973
- Rosahl S, Schell J, Willmitzer L (1987) Expression of a tuber-specific storage protein in transgenic tobacco plants: demonstration of an esterase activity. *EMBO J* **6**: 1155–1159
- Rzeznicka K, Walker CJ, Westergren T, Kannangara CG, von Wettstein D, Merchant S, Gough SP, Hansson M (2005) Xantha-I encodes a membrane subunit of the aerobic Mg-protoporphyrin IX monomethyl ester cyclase involved in chlorophyll biosynthesis. *Proc Natl Acad Sci USA* **102**: 5886–5891
- Schmidt GW, Delaney SK (2010) Stable internal reference genes for normalization of real-time RT-PCR in tobacco (*Nicotiana tabacum*) during development and abiotic stress. *Mol Genet Genomics* **283**: 233–241

- Schöttler MA, Flügel C, Thiele W, Stegemann S, Bock R (2007) The plastome-encoded Psaj subunit is required for efficient photosystem I excitation, but not for plastocyanin oxidation in tobacco. *Biochem J* **403**: 251–260
- Schöttler MA, Kirchhoff H, Weis E (2004) The role of plastocyanin in the adjustment of the photosynthetic electron transport to the carbon metabolism in tobacco. *Plant Physiol* **136**: 4265–4274
- Schult K, Meierhoff K, Paradies S, Töller T, Wolff P, Westhoff P (2007) The nuclear-encoded factor HCF173 is involved in the initiation of translation of the psbA mRNA in *Arabidopsis thaliana*. *Plant Cell* **19**: 1329–1346
- Schwenkert S, Netz DJ, Frazzon J, Pierik AJ, Bill E, Gross J, Lill R, Meurer J (2009) Chloroplast HCF101 is a scaffold protein for [4Fe-4S] cluster assembly. *Biochem J* **425**: 207–214
- Shalygo N, Czarnecki O, Peter E, Grimm B (2009) Expression of chlorophyll synthase is also involved in feedback-control of chlorophyll biosynthesis. *Plant Mol Biol* **71**: 425–436
- Stenbaek A, Hansson A, Wulff RP, Hansson M, Dietz KJ, Jensen PE (2008) NADPH-dependent thioredoxin reductase and 2-Cys peroxiredoxins are needed for the protection of Mg-protoporphyrin monomethyl ester cyclase. *FEBS Lett* **582**: 2773–2778
- Stöckel J, Oelmüller R (2004) A novel protein for photosystem I biogenesis. *J Biol Chem* **279**: 10243–10251
- Sun Q, Zybailov B, Majeran W, Friso G, Olinares PD, van Wijk KJ (2009) PPDB, the plant proteomics database at Cornell. *Nucleic Acids Res* **37**: D969–D974
- Tanaka R, Rothbart M, Oka S, Takabayashi A, Takahashi K, Shibata M, Myouga F, Motohashi R, Shinozaki K, Grimm B, et al (2010) LIL3, a light-harvesting-like protein, plays an essential role in chlorophyll and tocopherol biosynthesis. *Proc Natl Acad Sci USA* **107**: 16721–16725
- Tanaka R, Tanaka A (2007) Tetrapyrrole biosynthesis in higher plants. *Annu Rev Plant Biol* **58**: 321–346
- Tanaka R, Tanaka A (2011) Chlorophyll cycle regulates the construction and destruction of the light-harvesting complexes. *Biochim Biophys Acta* **1807**: 968–976
- Tottey S, Block MA, Allen M, Westergren T, Albrieux C, Scheller HV, Merchant S, Jensen PE (2003) Arabidopsis CHL27, located in both envelope and thylakoid membranes, is required for the synthesis of protochlorophyllide. *Proc Natl Acad Sci USA* **100**: 16119–16124
- Vandesompele J, De Preter K, Pattyn F, Poppe B, Van Roy N, De Paeppe A, Speleman F (2002) Accurate normalization of real-time quantitative RT-PCR data by geometric averaging of multiple internal control genes. *Genome Biol* **3**: research0034–research0034.11
- Waadt R, Schmidt LK, Lohse M, Hashimoto K, Bock R, Kudla J (2008) Multicolor bimolecular fluorescence complementation reveals simultaneous formation of alternative CBL/CIPK complexes in planta. *Plant J* **56**: 505–516
- Walker CJ, Castelfranco PA, Whyte BJ (1991) Synthesis of divinyl protochlorophyllide: enzymological properties of the Mg-protoporphyrin IX monomethyl ester oxidative cyclase system. *Biochem J* **276**: 691–697
- Wong YS, Castelfranco PA (1984) Resolution and reconstitution of Mg-protoporphyrin IX monomethyl ester (oxidative) cyclase, the enzyme system responsible for the formation of the chlorophyll isocyclic ring. *Plant Physiol* **75**: 658–661
- Zhang H, Goodman HM, Jansson S (1997) Antisense inhibition of the photosystem I antenna protein Lhca4 in *Arabidopsis thaliana*. *Plant Physiol* **115**: 1525–1531